

Supporting Information for :

**Fluorescent Molecular Rotors Based on Hinged Anthracene Carboxyimides**

Yanhui Ni,<sup>1</sup> Wangjian Fang,<sup>1</sup> and Mark A. Olson<sup>2,\*</sup>

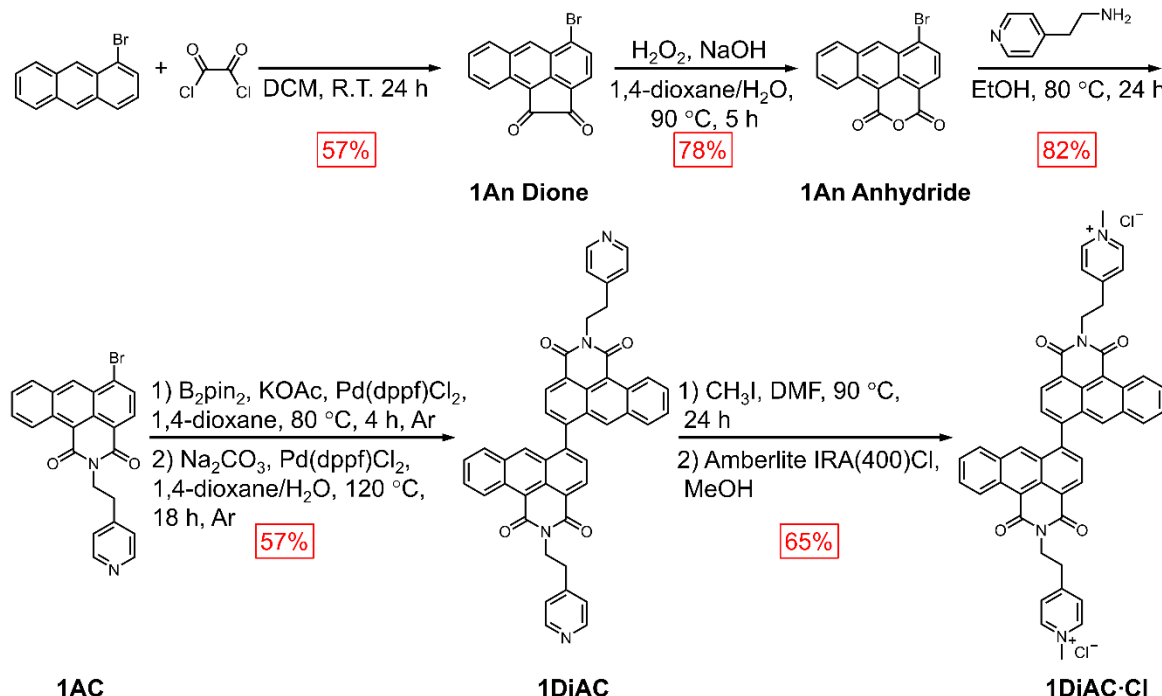
<sup>1</sup> *School of Pharmaceutical Science and Technology, Tianjin University, 92 Weijin Road, Nankai District, Tianjin, 300072, P. R. China.*

<sup>2</sup> *Department of Physical and Environmental Sciences, Texas A&M University Corpus Christi, Corpus Christi, TX. USA*

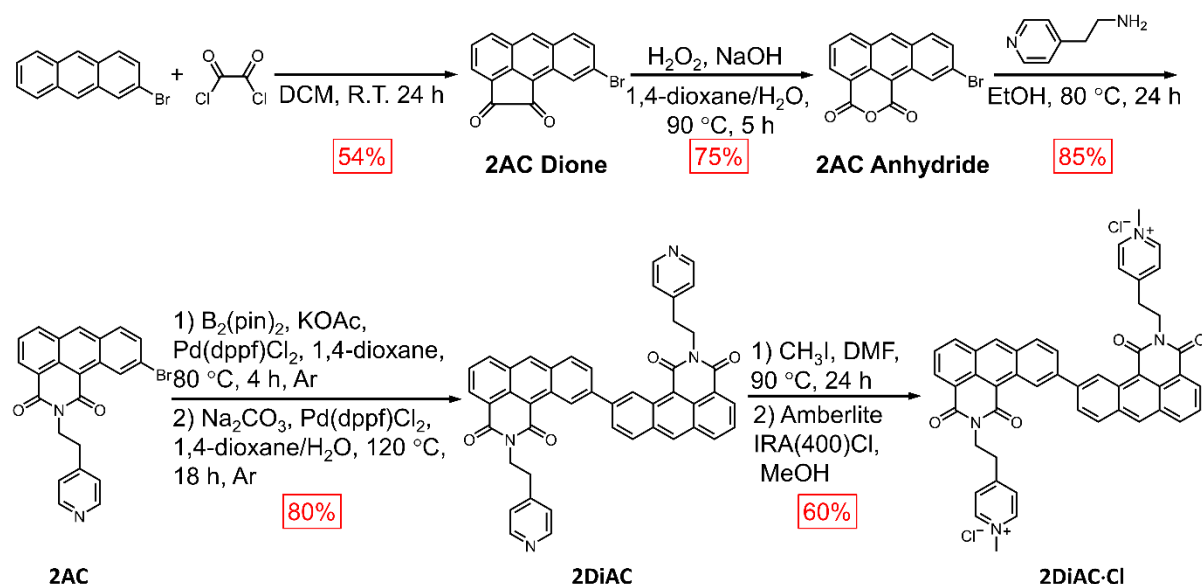
**Table of Contents**

1. Syntheses.....	2
2. Photophysical Properties and Solvatochromism.....	4
3. Multilinear Analysis Using Kamlet-Taft and Catalán Parameters .....	9
4. Viscosity Response of Fluorescent Molecular Rotors .....	11
5. Viscosity-Related Temperature Response of Fluorescent Molecular Rotors.....	13
6. Single Crystal Data .....	14
7. NMR Spectroscopic Characterization Data.....	16
8. High Resolution Mass Spectrometry Data.....	29
References.....	35

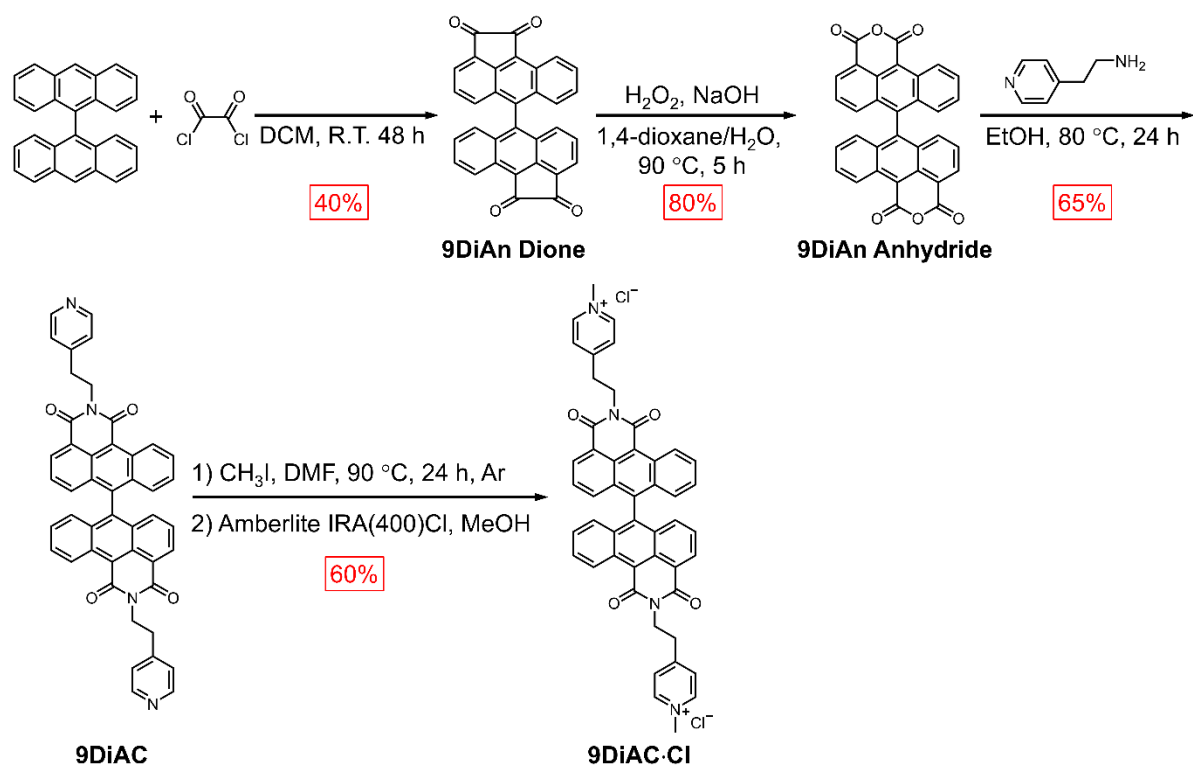
## 1. Syntheses



Scheme S1. The synthetic routes of the **1DiAC·Cl**.



Scheme S2. The synthetic routes of the **2DiAC·Cl**.



Scheme S3. The synthetic routes of the **9DiAC·Cl**.

## 2. Photophysical Properties and Solvatochromism

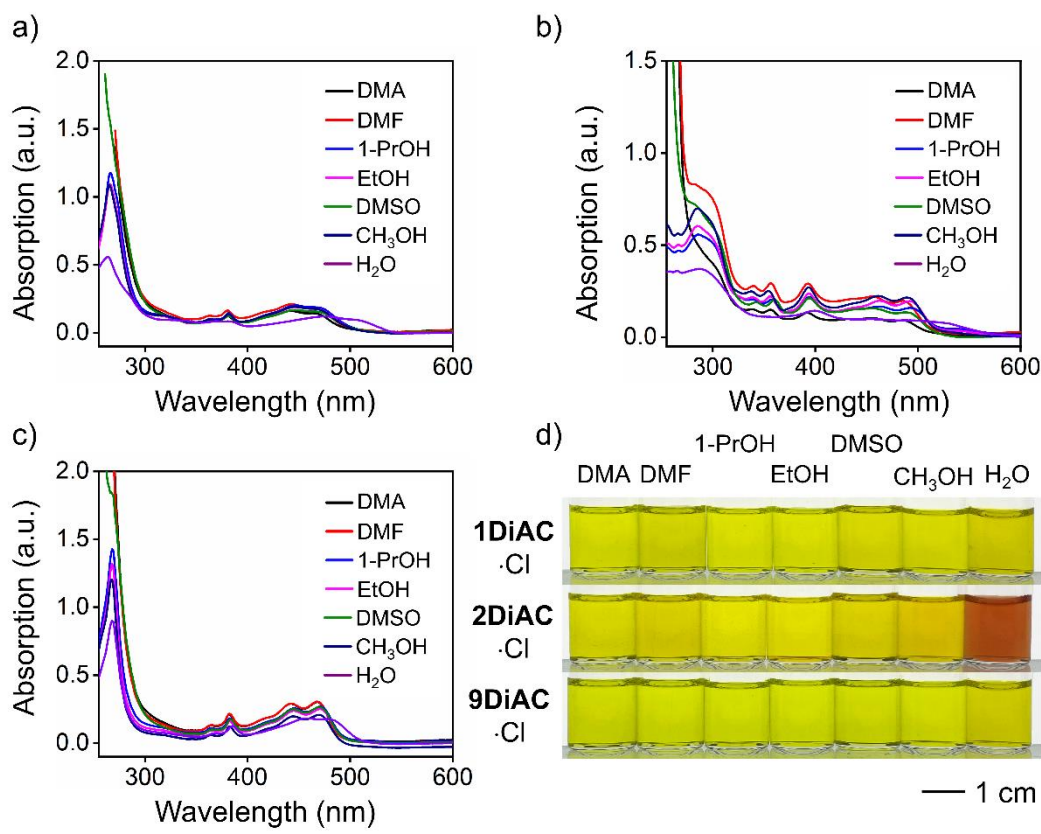


**Figure S1.** Absorption spectra of a) **1DiAC·Cl**, b) **2DiAC·Cl**, and c) **9DiAC·Cl** in various solvents ( $c = 1 \times 10^{-5}$  M). d) Photographs of 1 mM **1DiAC·Cl**, **2DiAC·Cl**, and **9DiAC·Cl** in N, N-dimethylacetamide (DMA), N, N-dimethylformamide (DMF), 1-propanol (1-PrOH), ethanol (EtOH), dimethyl sulfoxide (DMSO), methanol (CH<sub>3</sub>OH), and water (H<sub>2</sub>O).

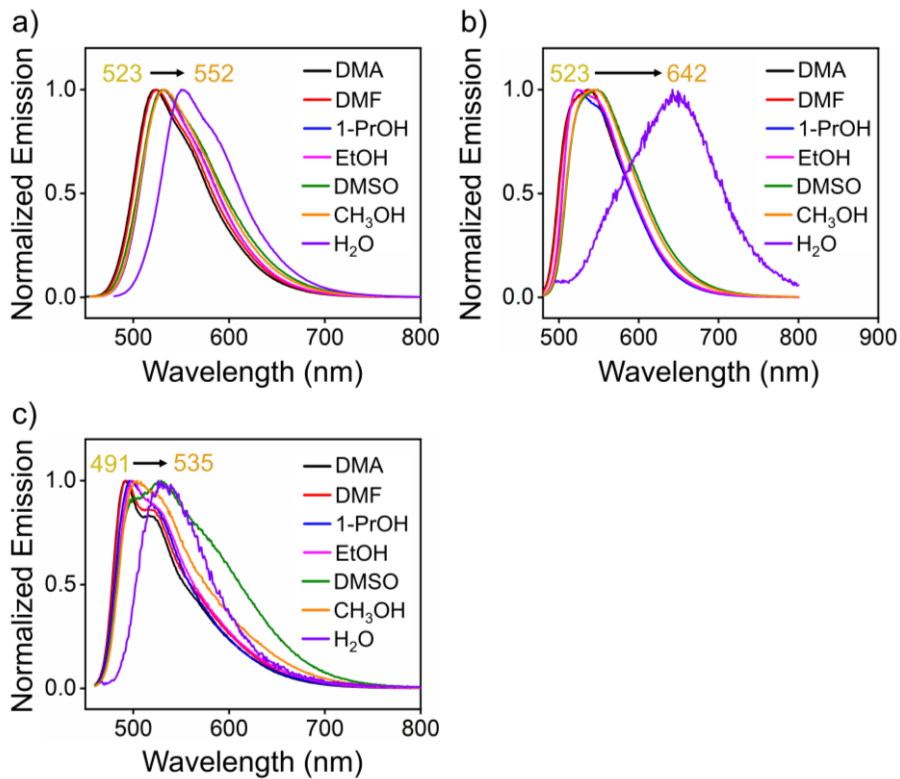


**Figure S2.** Normalized emission spectra of a) **1DiAC·Cl**, b) **2DiAC·Cl**, and c) **9DiAC·Cl** in various solvents ( $c = 1 \times 10^{-5}$  M).

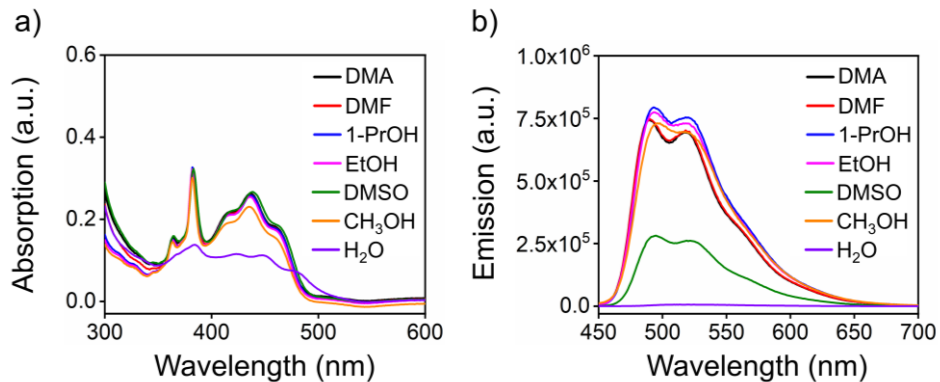


**Figure S3.** a) Absorption and b) emission spectra of **2AC** in N, N-dimethylacetamide (DMA), N, N-dimethylformamide (DMF), 1-propanol (1-PrOH), ethanol (EtOH), dimethyl sulfoxide (DMSO), methanol (CH<sub>3</sub>OH), and water (H<sub>2</sub>O).  $c = 1 \times 10^{-5}$  M.

**Table S1. Photophysical Data for the Excitation Center  $\lambda_{\text{Abs}}$ , Emission Center  $\lambda_{\text{Em}}$ , Stokes Shift ( $\Delta\nu_{\text{St}}$ ), the Absolute Quantum Yield ( $\Phi_F$ ), Fluorescent Lifetime ( $\tau$ ), and Molar Absorptivity ( $\epsilon_{\text{max}}$ ) of **1DiAC·Cl**, **2DiAC·Cl**, and **9DiAC·Cl** in Different Solvents.**

Parameters	DMA	DMF	1-PrOH	EtOH	DMSO	CH <sub>3</sub> OH	H <sub>2</sub> O
$\lambda_{\text{Abs}}$ of <b>1DiAC·Cl</b> / nm <sup>a</sup>	442	446	447	446	446	446	475
$\lambda_{\text{Em}}$ of <b>1DiAC·Cl</b> / nm <sup>a</sup>	522	524	531	531	531	532	552
$\Delta\nu_{\text{St}}/\text{cm}^{-1}$ <sup>b</sup>	3467	3338	3539	3589	3625	3625	2937
$\Phi_F$ of <b>1DiAC·Cl</b> <sup>c</sup>	0.6023	0.5187	0.4994	0.4512	0.2095	0.1396	0.1312
$\tau$ of <b>1DiAC·Cl</b> / ns	7.00	6.48	4.79	4.02	3.6	5.67	4.54
$\epsilon_{\text{max}} \times 10^4$ of <b>1DiAC·Cl</b> / M <sup>-1</sup> cm <sup>-1</sup>	1.61	2.1	2.01	1.89	1.68	1.91	1.21
$\lambda_{\text{Abs}}$ of <b>2DiAC·Cl</b> / nm <sup>a</sup>	456	456	464	463	456	461	489
$\lambda_{\text{Em}}$ of <b>2DiAC·Cl</b> / nm <sup>a</sup>	536	538	523	525	547	543	642
$\Delta\nu_{\text{St}}/\text{cm}^{-1}$ <sup>b</sup>	3273	3342	2431	2551	3648	3276	4874
$\Phi_F$ of <b>2DiAC·Cl</b> <sup>c</sup>	0.6801	0.6092	0.6032	0.5782	0.4103	0.2825	0.0081
$\tau$ of <b>2DiAC·Cl</b> / ns	7.28	6.02	5.32	5.87	5.38	5.01	5.19
$\epsilon_{\text{max}} \times 10^4$ of <b>2DiAC·Cl</b> / M <sup>-1</sup> cm <sup>-1</sup>	1.04	2.21	1.67	1.98	1.56	2.24	0.92
$\lambda_{\text{Abs}}$ of <b>9DiAC·Cl</b> / nm <sup>a</sup>	442	442	446	445	445	444	458
$\lambda_{\text{Em}}$ of <b>9DiAC·Cl</b> / nm <sup>a</sup>	491	492	498	500	498	505	535
$\Delta\nu_{\text{St}}/\text{cm}^{-1}$ <sup>b</sup>	2258	2299	2341	2472	2392	2721	3142
$\Phi_F$ of <b>9DiAC·Cl</b> <sup>c</sup>	0.2536	0.1643	0.1525	0.1234	0.0642	0.0018	0.0001
$\tau$ of <b>9DiAC·Cl</b> / ns	7.06	6.95	3.71	3.41	4.87	6.00	6.66
$\epsilon_{\text{max}} \times 10^4$ of <b>1DiAC·Cl</b> / M <sup>-1</sup> cm <sup>-1</sup>	2.89	2.91	2.56	2.38	2.49	1.96	1.82

<sup>a</sup>All spectra in solution were measured using a 1 cm path length quartz cuvette at a concentration of  $1 \times 10^{-5}$  M at 298 K. <sup>b</sup>  $\Delta\nu_{\text{St}} = \nu_{\text{Abs}_{\text{max}}} - \nu_{\text{Em}_{\text{max}}}$ . <sup>c</sup>  $\Phi$  = Absolute fluorescence quantum yield obtained using an integrating sphere.

**Table S2. Photophysical Data for the Excitation Center  $\lambda_{\text{Abs}}$ , Emission Center  $\lambda_{\text{Em}}$ , Stokes Shift ( $\Delta\nu_{\text{St}}$ ), and Molar Absorptivity ( $\epsilon_{\text{max}}$ ) of 2AC in Different Solvents.**

Parameters	DMA	DMF	1-PrOH	EtOH	DMSO	CH <sub>3</sub> OH	H <sub>2</sub> O
$\lambda_{\text{Abs}}$ of <b>2AC</b> / nm <sup>a</sup>	382	381	382	382	383	382	384
$\lambda_{\text{Em}}$ of <b>2AC</b> / nm <sup>a</sup>	490	490	493	494	495	496	522
$\Delta\nu_{\text{St}}/\text{cm}^{-1}$ <sup>b</sup>	5770	5839	5894	5935	5907	6016	6885
$\epsilon_{\text{max}} \times 10^4$ of <b>2AC</b> / M <sup>-1</sup> cm <sup>-1</sup>	1.05	1.03	1.09	1.07	1.08	1.00	1.06

<sup>a</sup>All spectra in solution were measured using a 1 cm path length quartz cuvette at a concentration of  $1 \times 10^{-5}$  M at 298 K. <sup>b</sup>  $\Delta\nu_{\text{St}} = \nu_{\text{Abs}_{\text{max}}} - \nu_{\text{Em}_{\text{max}}}$ .

**Table S3. Dielectric constant ( $\epsilon$ ), Refractive Index of the Solvent (n), and Orientation Polarizability ( $\Delta f$ ) of solvents.**

Parameters	DMA	DMF	1-PrOH	EtOH	DMSO	CH <sub>3</sub> OH	H <sub>2</sub> O
$\epsilon$	38.3	36.7	20.45	24.55	46.68	32.6	78.36
n	1.438	1.43	1.384	1.359	1.479	1.327	1.34
$\Delta f$	0.794	0.793	0.749	0.777	0.797	0.812	0.858

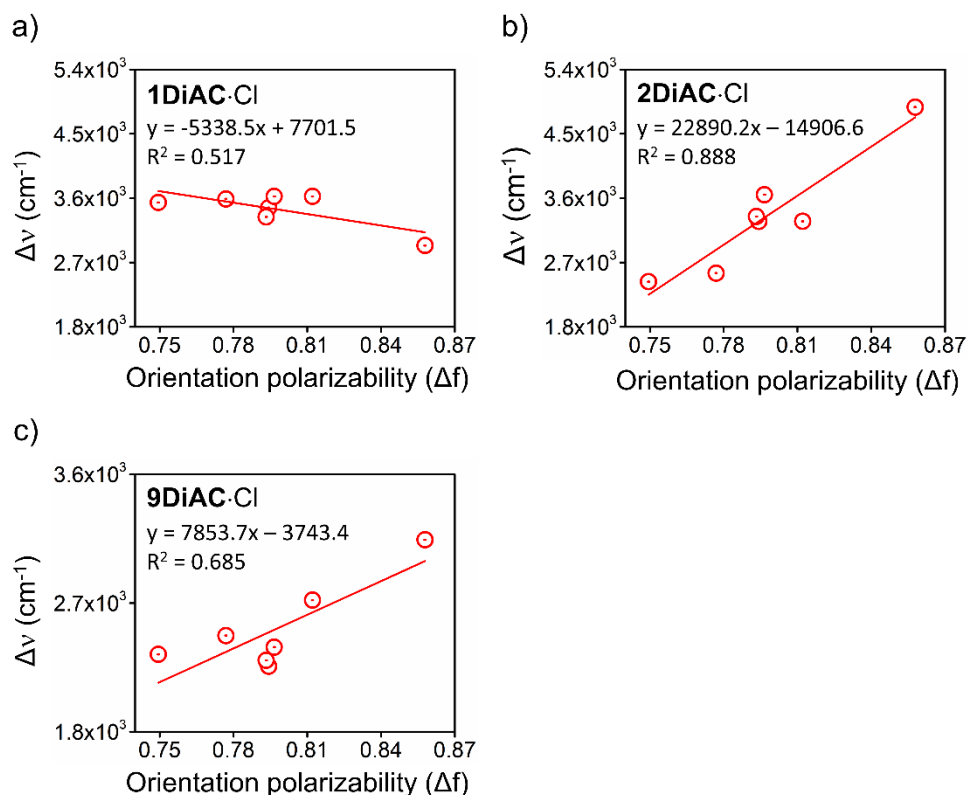


**Figure S4.** Lippert-Mataga plots for a) **1DiAC·Cl**, b) **2DiAC·Cl**, and c) **9DiAC·Cl**.

### 3. Multilinear Analysis Using Kamlet-Taft and Catalán Parameters

**Table S4. The Physical Parameters of the Solvents (Kamlet-Taft and Catalán).**

Solvent	Kamlet-Taft Parameter			Catalan Parameter			
	$\alpha$	$\beta$	$\pi^*$	SA	SB	SP	SDP
N, N-dimethylacetamide	0	0.76	0.88	0.028	0.65	0.763	0.987
N, N-dimethylformamide	0	0.69	0.88	0.031	0.613	0.759	0.977
1-propanol	0.76	0.84	0.48	0.367	0.782	0.658	0.748
ethanol	0.86	0.75	0.54	0.4	0.658	0.633	0.783
dimethyl sulfoxide	0	0.76	1	0.072	0.647	0.83	1
methanol	0.98	0.66	0.6	0.605	0.545	0.608	0.904
water	1.17	0.47	1.09	1.062	0.025	0.681	0.997

**Table S5. Estimated Coefficients ( $y_0$ ,  $a_\alpha$ ,  $b_\beta$ ,  $c_{\pi^*}$ ), Their Standard Errors, and Regression Coefficients ( $R^2$ ) for the multilinear analysis of  $\nu_{\text{Abs}}$ ,  $\nu_{\text{Em}}$ ,  $\Delta\nu_{\text{St}}$ , and  $\Phi_F$  of Investigated Rotors in N, N-dimethylacetamide (DMA), N, N-dimethylformamide (DMF), 1-propanol (1-PrOH), ethanol (EtOH), dimethyl sulfoxide (DMSO), methanol (CH<sub>3</sub>OH), and water (H<sub>2</sub>O) as a Function of Kamlet-Taft Solvent Scalesb.**

Parameters	$y_0 / \text{cm}^{-1}$	$a_\alpha$	$b_\beta$	$c_{\pi^*}$	$R^2$
$\nu_{\text{Abs}}$ of <b>1DiAC·Cl</b>	$24890 \pm 2270$	$-1008 \pm 390$	$-689 \pm 1994$	$-2066 \pm 919$	0.839
$\nu_{\text{Em}}$ of <b>1DiAC·Cl</b>	$20915 \pm 898$	$-765 \pm 154$	$-866 \pm 788$	$-1376 \pm 363$	0.936
$\Delta\nu_{\text{St}}$ of <b>1DiAC·Cl</b>	$3975 \pm 2109$	$-243 \pm 363$	$177 \pm 1852$	$-689 \pm 854$	0.291
$\Phi_F$ of <b>1DiAC·Cl</b>	$1.11 \pm 2.03$	$-0.30 \pm 0.35$	$-0.22 \pm 1.78$	$-0.54 \pm 0.82$	0.53
$\nu_{\text{Abs}}$ of <b>2DiAC·Cl</b>	$24609 \pm 2330$	$-1196 \pm 400$	$-1285 \pm 2046$	$-1890 \pm 944$	0.825
$\nu_{\text{Em}}$ of <b>2DiAC·Cl</b>	$22611 \pm 2171$	$-1685 \pm 373$	$-319 \pm 1906$	$-4718 \pm 879$	0.972
$\Delta\nu_{\text{St}}$ of <b>2DiAC·Cl</b>	$1999 \pm 1608$	$489 \pm 276$	$-1603 \pm 1412$	$2827 \pm 651$	0.965
$\Phi_F$ of <b>2DiAC·Cl</b>	$1.18 \pm 1.23$	$-0.39 \pm 0.21$	$0.06 \pm 1.08$	$-0.72 \pm 0.50$	0.88
$\nu_{\text{Abs}}$ of <b>9DiAC·Cl</b>	$24989 \pm 951$	$-731 \pm 163$	$-1489 \pm 835$	$-1436 \pm 385$	0.891
$\nu_{\text{Em}}$ of <b>9DiAC·Cl</b>	$22741 \pm 617$	$-1221 \pm 106$	$-838 \pm 542$	$-2031 \pm 250$	0.990
$\Delta\nu_{\text{St}}$ of <b>9DiAC·Cl</b>	$2248 \pm 571$	$490 \pm 98$	$-651 \pm 502$	$594 \pm 231$	0.971
$\Phi_F$ of <b>9DiAC·Cl</b>	$0.25 \pm 0.91$	$-0.13 \pm 0.16$	$0.06 \pm 0.80$	$-0.14 \pm 0.37$	0.57

**Table S6. Estimated Coefficients ( $y_0$ ,  $a_{SA}$ ,  $b_{SB}$ ,  $c_{SP}$ ,  $d_{SDP}$ ), Their Standard Errors, and Regression Coefficients ( $R^2$ ) for the multilinear analysis of  $\nu_{Abs}$ ,  $\nu_{Em}$ ,  $\Delta\nu_{St}$ , and  $\Phi_F$  of Investigated Rotors in N,N-dimethylacetamide (DMA), N,N-dimethylformamide (DMF), 1-propanol (1-PrOH), ethanol (EtOH), dimethyl sulfoxide (DMSO), methanol (CH<sub>3</sub>OH), and water (H<sub>2</sub>O) as a Function of Catalán Solvent Scales.**

Parameters	$y_0 / \text{cm}^{-1}$	$a_{SA}$	$b_{SB}$	$c_{SP}$	$d_{SDP}$	$R^2$
$\nu_{Abs}$ of <b>1DiAC·Cl</b>	$20904 \pm 1739$	$-395 \pm 519$	$2304 \pm 790$	$-3453 \pm 1199$	$2879 \pm 1057$	0.962
$\nu_{Em}$ of <b>1DiAC·Cl</b>	$20892 \pm 1155$	$-1196 \pm 345$	$-77 \pm 525$	$-2554 \pm 796$	$227 \pm 701$	0.958
$\Delta\nu_{St}$ of <b>1DiAC·Cl</b>	$13 \pm 2053$	$801 \pm 613$	$2380 \pm 933$	$-898 \pm 1416$	$2652 \pm 1248$	0.733
$\Phi_F$ of <b>1DiAC·Cl</b>	$5.05 \pm 2.45$	$-1.54 \pm 0.73$	$-1.84 \pm 1.12$	$-1.25 \pm 1.69$	$-2.42 \pm 1.49$	0.82
$\nu_{Abs}$ of <b>2DiAC·Cl</b>	$19177 \pm 1849$	$-405 \pm 552$	$2208 \pm 840$	$-2602 \pm 1274$	$3449 \pm 1123$	0.956
$\nu_{Em}$ of <b>2DiAC·Cl</b>	$21582 \pm 2089$	$-1662 \pm 624$	$3051 \pm 950$	$-6244 \pm 1440$	$-45 \pm 1269$	0.990
$\Delta\nu_{St}$ of <b>2DiAC·Cl</b>	$-2405 \pm 875$	$1257 \pm 261$	$-843 \pm 397$	$3642 \pm 603$	$3494 \pm 531$	0.996
$\Phi_F$ of <b>2DiAC·Cl</b>	$3.68 \pm 1.36$	$-1.21 \pm 0.41$	$-0.93 \pm 0.62$	$-1.11 \pm 0.94$	$-1.62 \pm 0.83$	0.96
$\nu_{Abs}$ of <b>9DiAC·Cl</b>	$22734 \pm 434$	$-608 \pm 130$	$673 \pm 197$	$-2727 \pm 299$	$1595 \pm 264$	0.991
$\nu_{Em}$ of <b>9DiAC·Cl</b>	$21483 \pm 566$	$-1479 \pm 169$	$-583 \pm 257$	$-2782 \pm 390$	$656 \pm 344$	0.997
$\Delta\nu_{St}$ of <b>9DiAC·Cl</b>	$1251 \pm 982$	$871 \pm 293$	$90 \pm 3446$	$55 \pm 677$	$939 \pm 597$	0.976
$\Phi_F$ of <b>9DiAC·Cl</b>	$1.77 \pm 1.39$	$-0.61 \pm 0.41$	$-0.68 \pm 0.63$	$-0.41 \pm 0.96$	$-0.84 \pm 0.84$	0.74

**Table S7. Percentage Contribution of the Solvatochromic Parameters (Catalán Equation) Using Absorption, Emission Frequencies, and Absolute Fluorescent Quantum Yield.**

Parameters	P <sub>SA</sub> / %	P <sub>SB</sub> / %	P <sub>SP</sub> / %	P <sub>SDP</sub> / %
$\nu_{Abs}$ of <b>1DiAC·Cl</b>	4.37	25.51	38.23	31.88
$\nu_{Em}$ of <b>1DiAC·Cl</b>	29.50	1.90	63.00	5.60
$\Phi_F$ of <b>1DiAC·Cl</b>	21.84	26.10	17.73	34.33
$\nu_{Abs}$ of <b>2DiAC·Cl</b>	4.67	25.48	30.03	39.81
$\nu_{Em}$ of <b>2DiAC·Cl</b>	15.11	27.73	56.75	0.41
$\Phi_F$ of <b>2DiAC·Cl</b>	24.85	19.09	22.79	33.26
$\nu_{Abs}$ of <b>9DiAC·Cl</b>	10.85	12.01	48.67	28.47
$\nu_{Em}$ of <b>9DiAC·Cl</b>	26.89	10.60	50.58	11.93
$\Phi_F$ of <b>9DiAC·Cl</b>	24.02	26.77	16.14	33.07

#### 4. Viscosity Response of Fluorescent Molecular Rotors

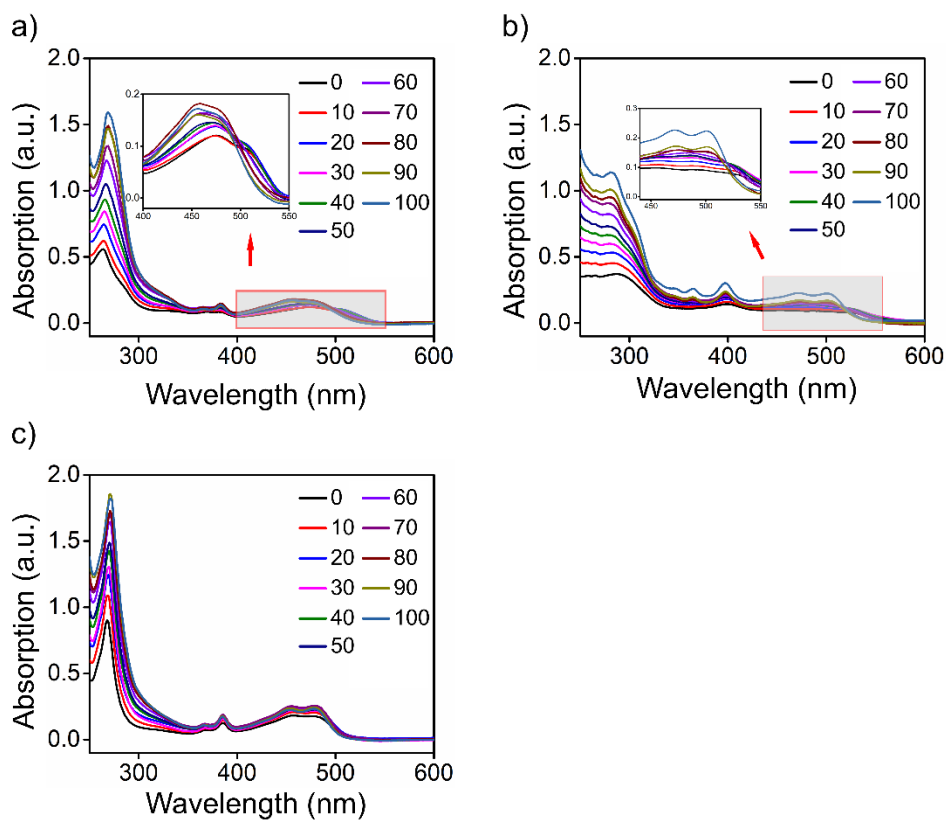


**Figure S5.** Absorption spectra of a) **1DiAC·Cl**, b) **2DiAC·Cl**, and c) **9DiAC·Cl** binary mixtures of water and glycerol in different ratios.  $c = 1 \times 10^{-5}$  M.

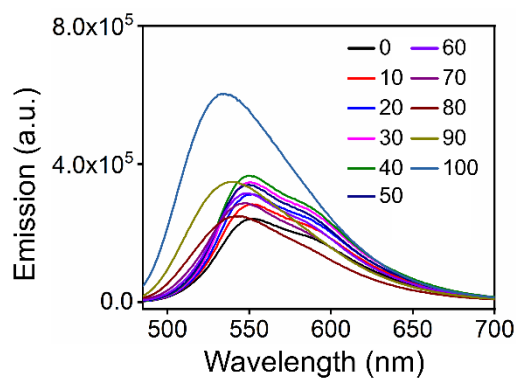


**Figure S6.** Emission spectra of **1DiAC·Cl** in binary mixtures of water and glycerol in different ratios.  $c = 1 \times 10^{-5}$  M.

**Table S8. Viscosity in Different Fractions of Glycerol in Water at 25 °C.**

Volume Fraction /%	Viscosity / mPa·s
0	0.89
10	1.17
20	1.58
30	2.16
40	3.25
50	5.04
60	10.6
70	17.95
80	46.7
90	168.6
100	956.1

## 5. Viscosity-Related Temperature Response of Fluorescent Molecular Rotors

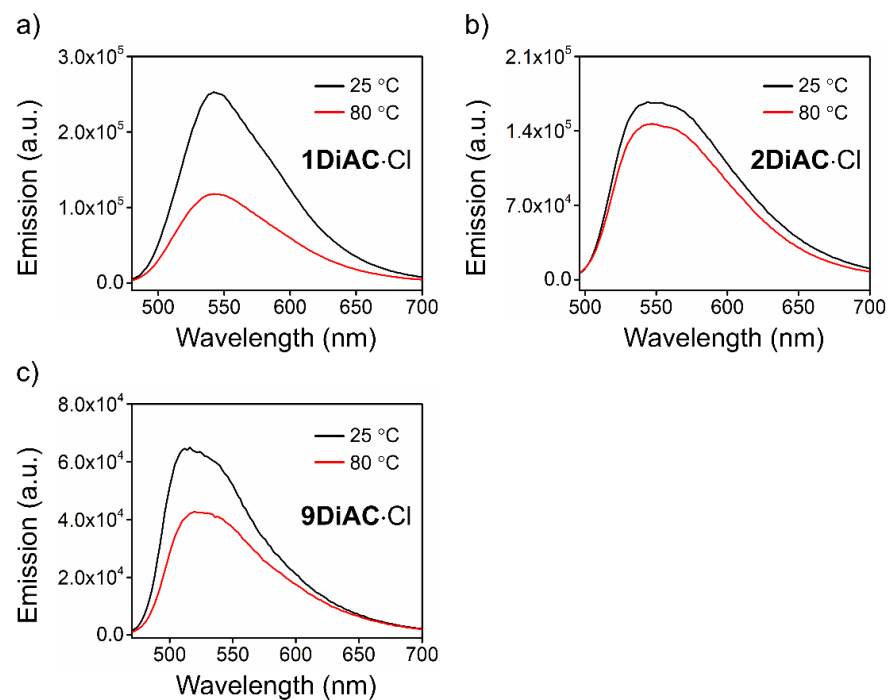


**Figure S7.** Emission spectra of a) **1DiAC·Cl**, b) **2DiAC·Cl**, and c) **9DiAC·Cl** in binary mixtures of water and glycerol ( $v:v = 2:8$ ,  $c = 1 \times 10^{-5}$  M) at 25 and 80 °C.

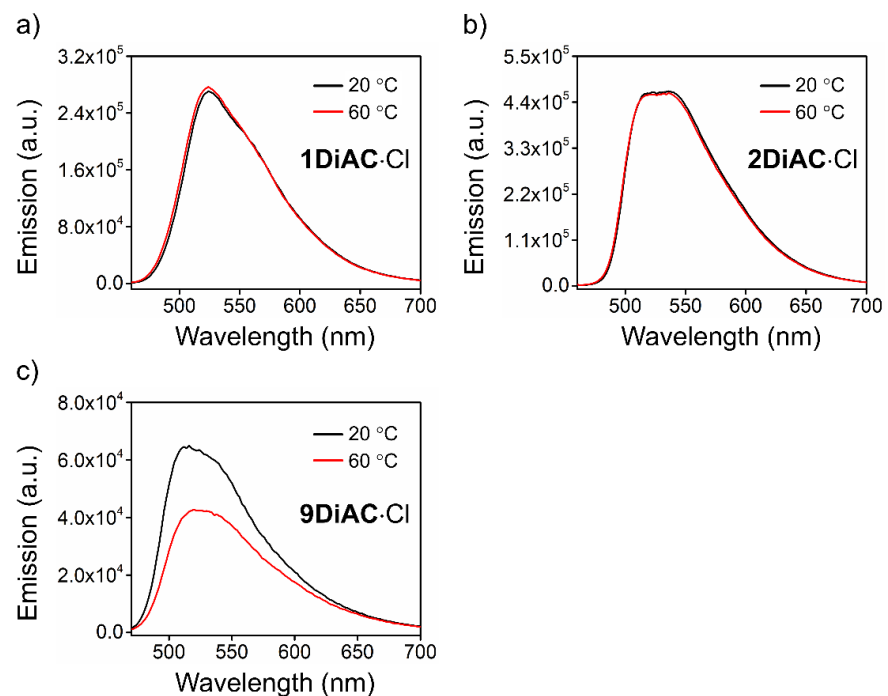


**Figure S8.** Emission spectra of a) **1DiAC·Cl**, b) **2DiAC·Cl**, and c) **9DiAC·Cl** in DMF ( $c = 1 \times 10^{-5}$  M) at 20 and 60 °C.

## 6. Single Crystal Data

Single crystals suitable for X-ray diffraction were selected and X-ray diffraction intensity data was collected on a Rigaku XtaLAB FRX diffractometer equipped with a Hypix6000HE detector and Rigaku MM-007 rotating anode diffractometer equipped with a Rigaku Pilatus 200K hybrid photon counting detector, using Cu K $\alpha$  radiation ( $\lambda = 1.54184 \text{ \AA}$ ). **9DiAC·PF<sub>6</sub>** crystals were grown from slow evaporation from dichloromethane and acetonitrile. Using Olex2,<sup>[1]</sup> structures were solved either with the ShelXT<sup>[2]</sup> by direct methods. The hydrogen atoms were set in calculated positions and refined as riding atoms with a common fixed isotropic thermal parameter. More details of the data collection and structural refinement of all molecules can be found in Tables S7.

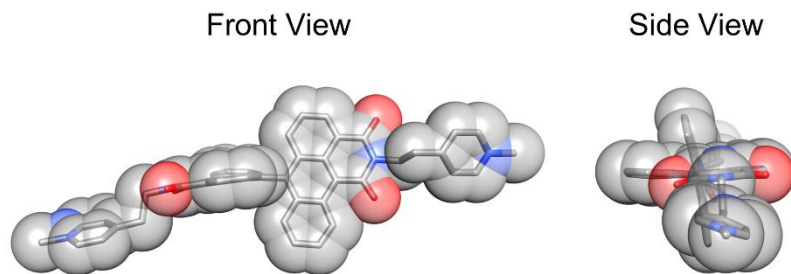


**Figure S9.** Mixed space filling and stick representations of the X-ray crystal structures of **9DiAC·PF<sub>6</sub>** as viewed from the front and the side. Hydrogen atoms and counterions have been omitted for clarity.

**Table S9. Crystallographic Parameters for 9DiAC·PF<sub>6</sub>.**

Empirical formula	C <sub>30</sub> H <sub>26</sub> N <sub>4</sub> O <sub>4</sub>
Formula weight	506.55
Temperature/K	293(2)
Crystal system	monoclinic
Space group	P2 <sub>1</sub> /n
a/Å	12.6741(2)
b/Å	13.4071(2)
c/Å	16.1884 (3)
α/°	90
β/°	90.2360 (10)
γ/°	90
Volume/Å <sup>3</sup>	2750.76(8)
Z	4
ρ <sub>calcg</sub> /cm <sup>3</sup>	1.223
μ/mm <sup>-1</sup>	0.672
F(000)	1064.0
Crystal size/mm <sup>3</sup>	0.3 × 0.2 × 0.2
Radiation	Cu Kα ( $\lambda = 1.54184$ )
2θ range for data collection/°	8.844 to 133.194
Index ranges	-14 ≤ h ≤ 15, -15 ≤ k ≤ 15, -19 ≤ l ≤ 16
Reflections collected	11657
Independent reflections	4616 [R <sub>int</sub> = 0.0187, R <sub>sigma</sub> = 0.0219]
Data/restraints/parameters	4616/0/343
Goodness-of-fit on F <sup>2</sup>	1.054
Final R indexes [I>=2σ (I)]	R <sub>1</sub> = 0.0616, wR <sub>2</sub> = 0.1806
Final R indexes [all data]	R <sub>1</sub> = 0.0669, wR <sub>2</sub> = 0.1867
Largest diff. peak/hole / e Å <sup>-3</sup>	0.23/-0.32
CCDC No.	2203337

## 7. NMR Spectroscopic Characterization Data

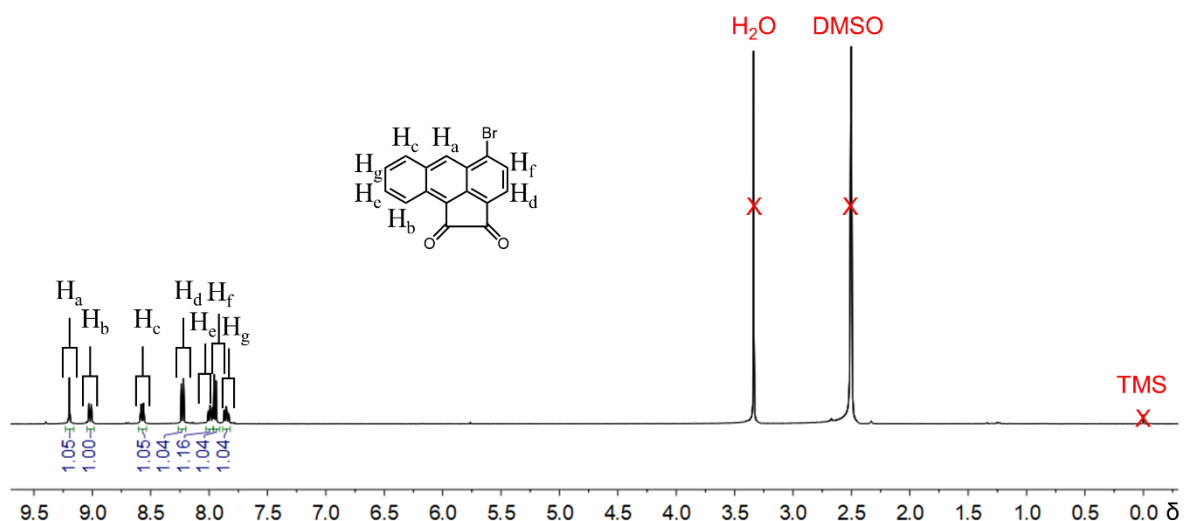


**Figure S10.**  $^1\text{H}$  NMR spectrum of **1An Dione** (400 MHz, DMSO-d<sub>6</sub>, 298 K).

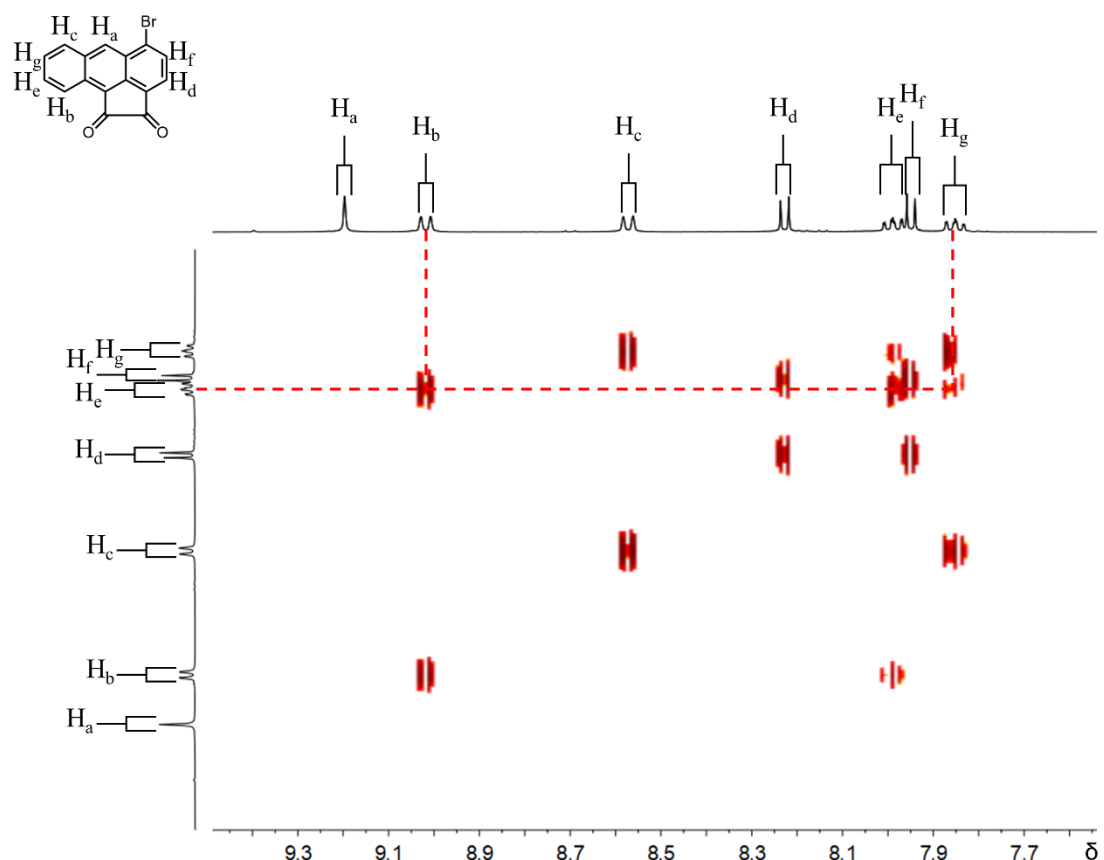


**Figure S11.**  $^1\text{H}$ - $^1\text{H}$  COSY NMR spectrum of **1An Dione** (400 MHz, DMSO-d<sub>6</sub>, 298 K).

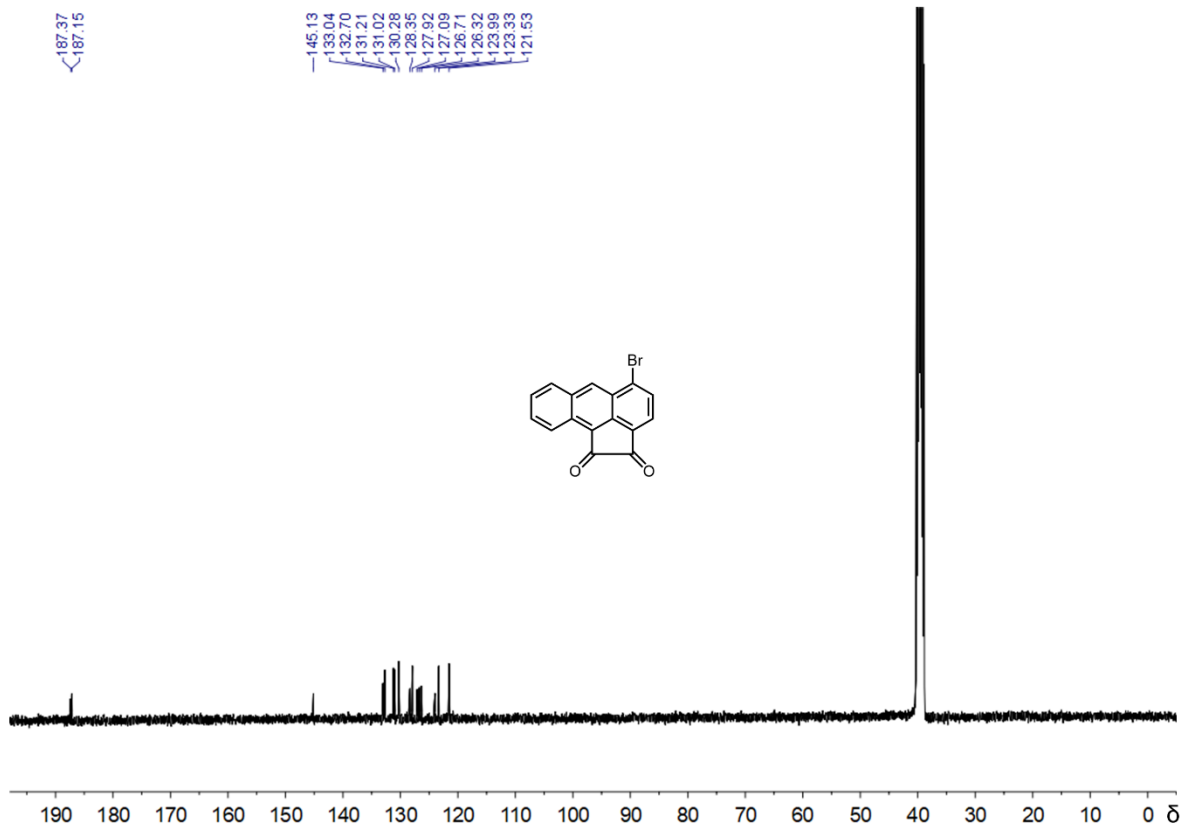


**Figure S12.** <sup>13</sup>C NMR Spectrum of **1An Dione** (101 MHz, DMSO-d<sub>6</sub>, 298 K).

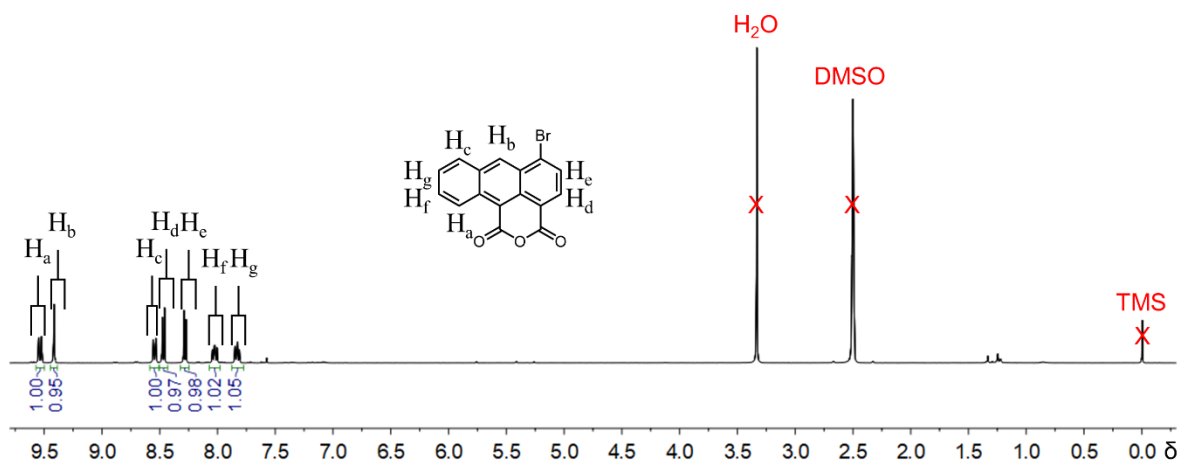


**Figure S13.** <sup>1</sup>H NMR spectrum of **1An Anhydride** (400 MHz, DMSO-d<sub>6</sub>, 298 K).

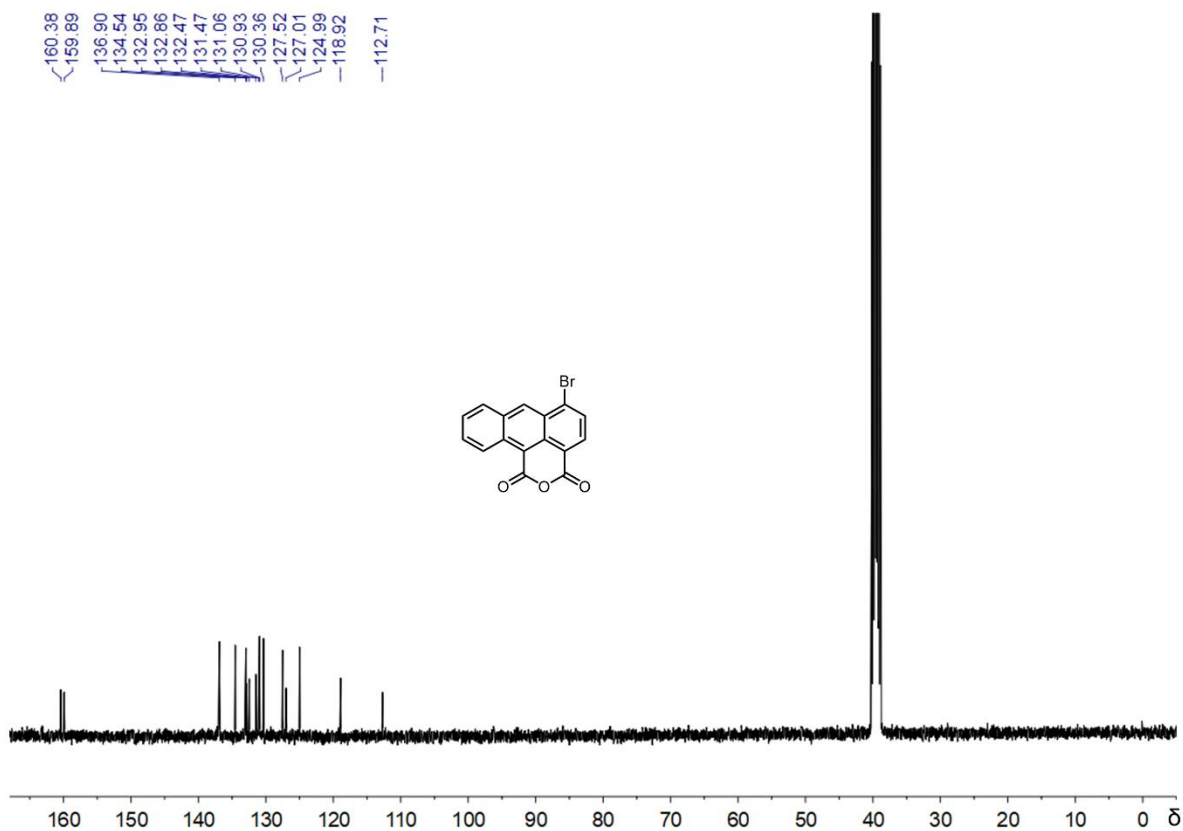


**Figure S14.**  $^{13}\text{C}$  NMR Spectrum of **1An** Anhydride (101 MHz, DMSO-d6, 298 K).

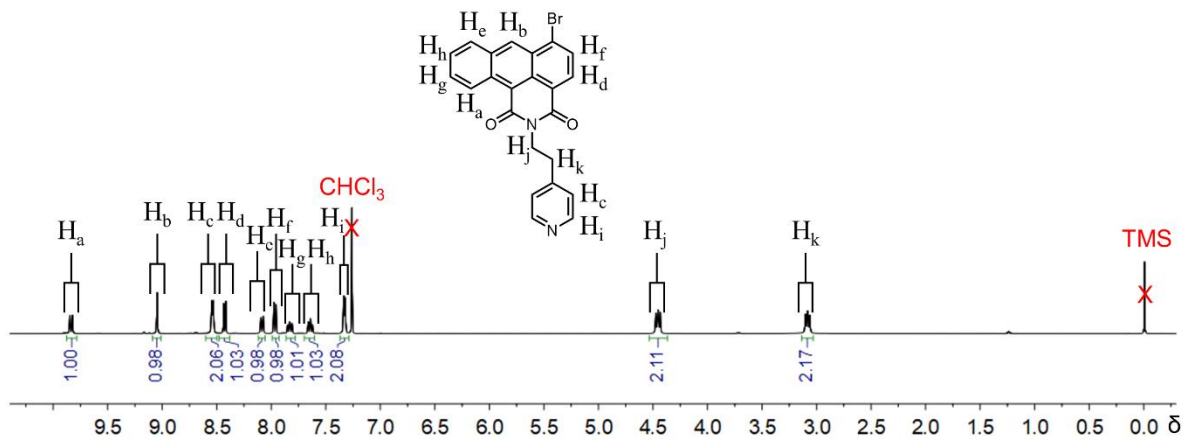


**Figure S15.**  $^1\text{H}$  NMR spectrum of **1AC** (400 MHz,  $\text{CDCl}_3$ , 298 K).

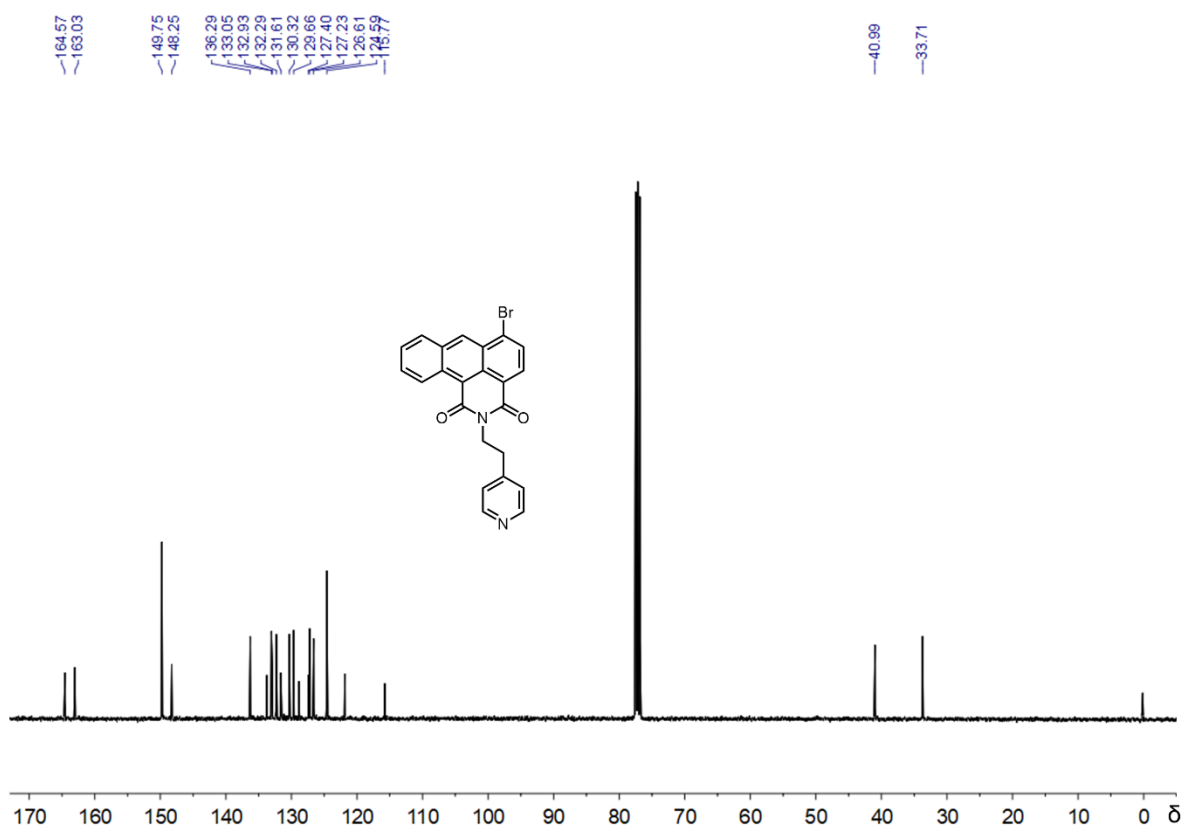


**Figure S16.**  $^{13}\text{C}$  NMR Spectrum of **1AC** (101 MHz,  $\text{CDCl}_3$ , 298 K).

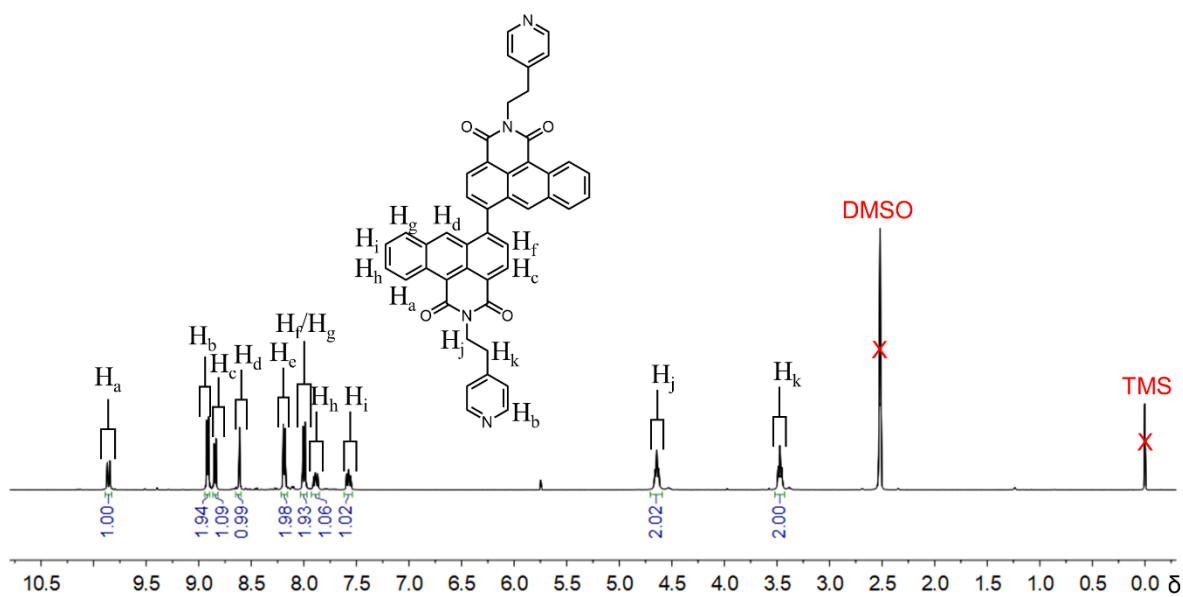


**Figure S17.**  $^1\text{H}$  NMR spectrum of **1DiAC** (400 MHz,  $\text{DMSO-d}_6$ , 298 K).

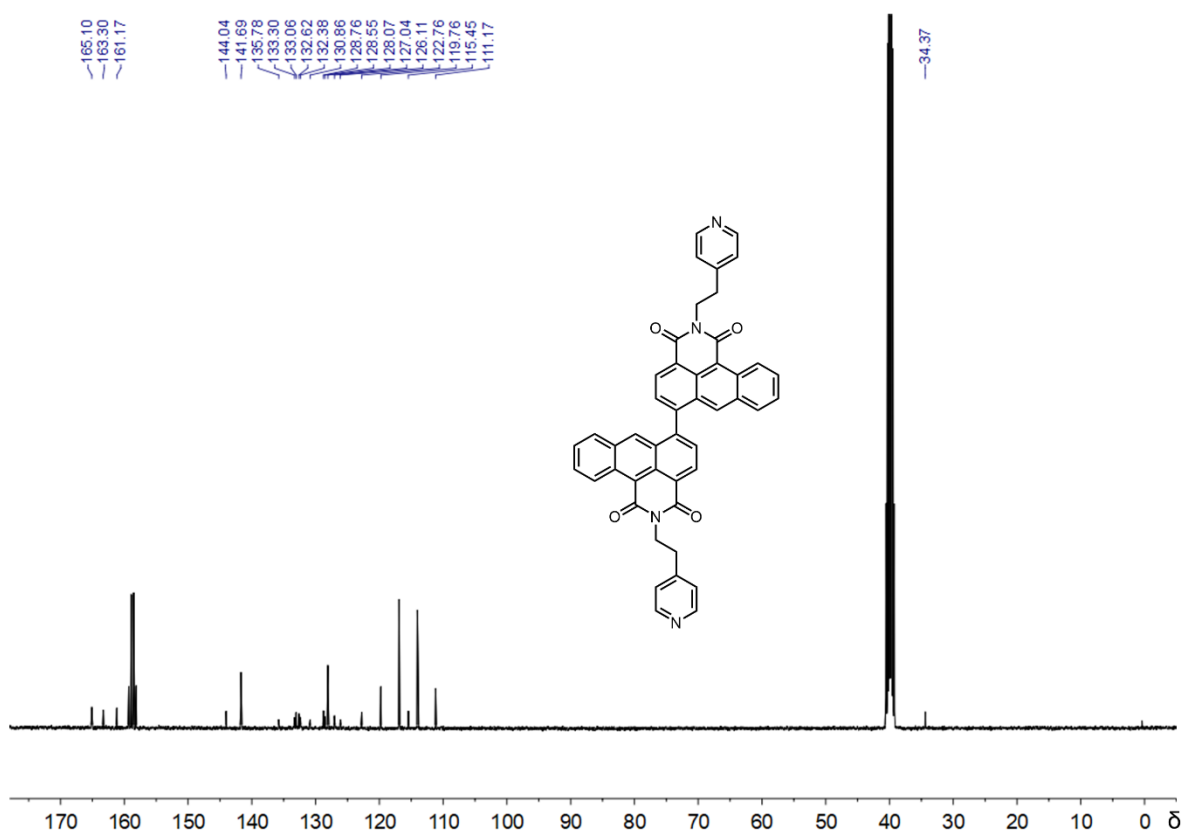


**Figure S18.**  $^{13}\text{C}$  NMR Spectrum of **1DiAC** (101 MHz, DMSO-d<sub>6</sub>, 298 K).

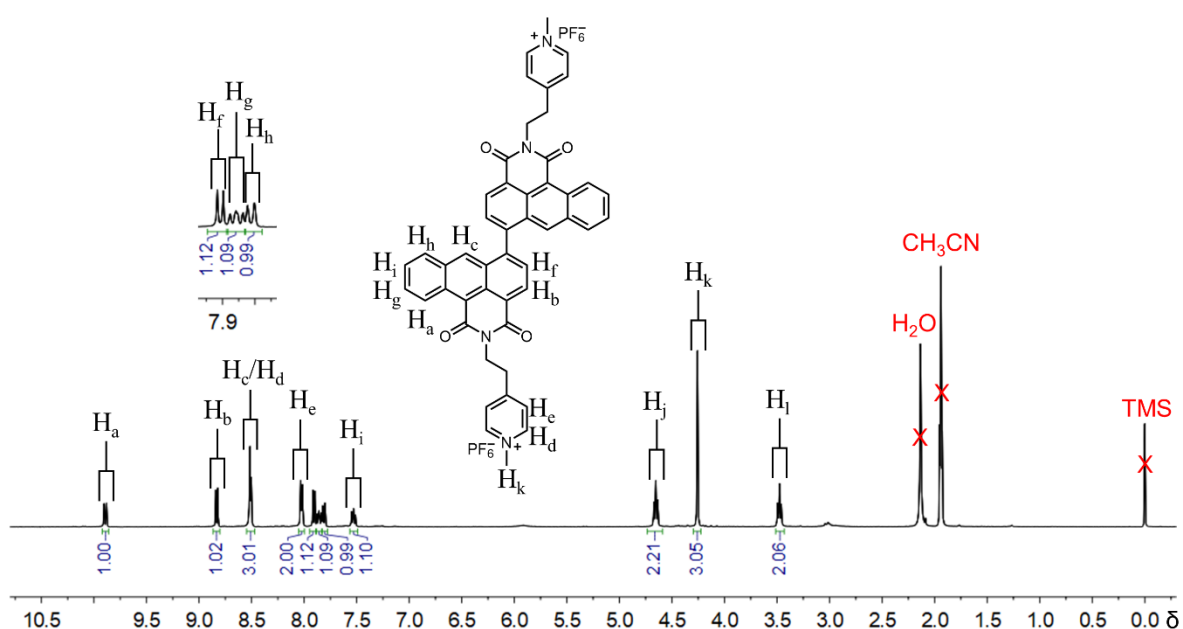


**Figure S19.**  $^1\text{H}$  NMR spectrum of **1DiAC·PF<sub>6</sub>** (400 MHz, CD<sub>3</sub>CN, 298 K).

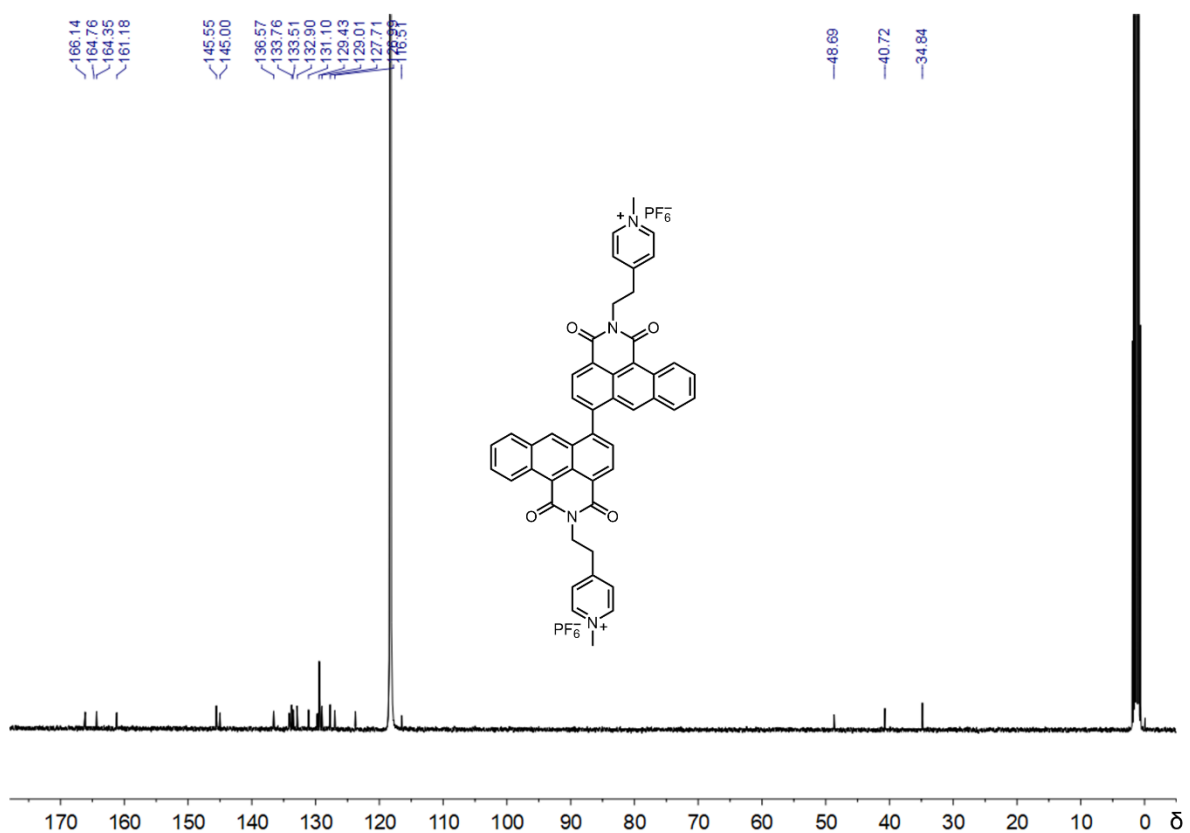


**Figure S20.**  $^{13}\text{C}$  NMR Spectrum of **1DiAC·PF<sub>6</sub>** (101 MHz, CD<sub>3</sub>CN, 298 K).

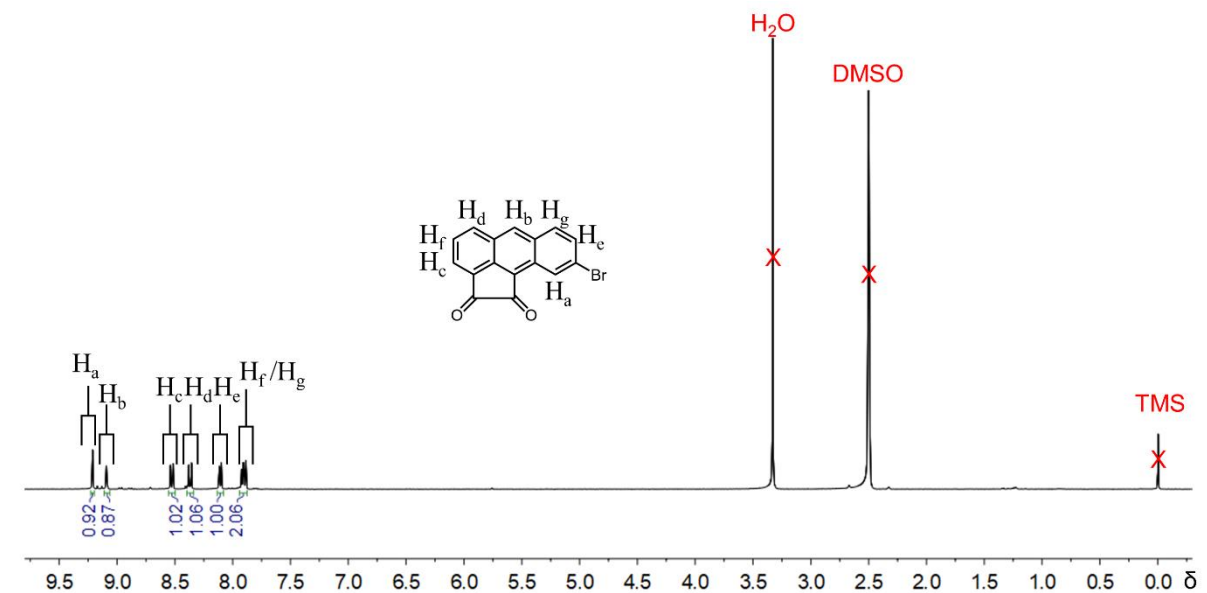


**Figure S21.**  $^1\text{H}$  NMR spectrum of **2An Dione** (400 MHz, DMSO-d<sub>6</sub>, 298 K).

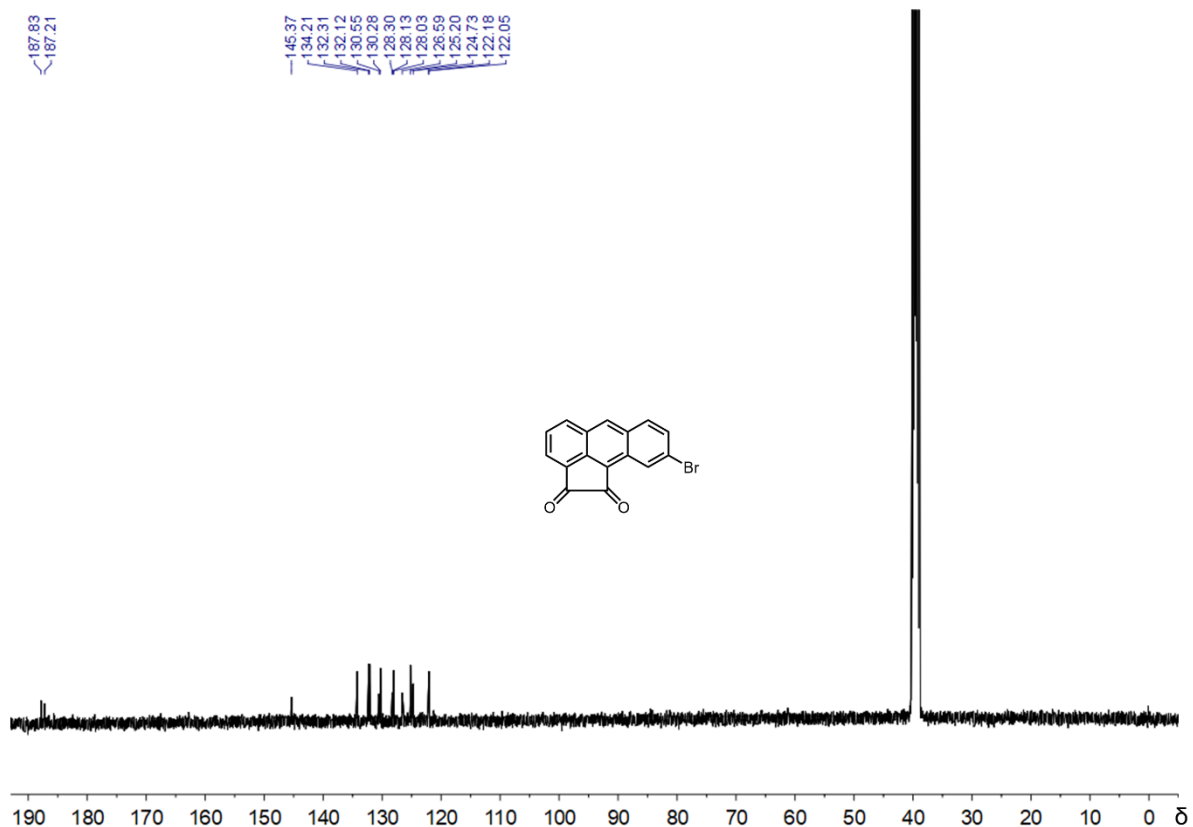


**Figure S22.**  $^{13}\text{C}$  NMR Spectrum of 2An Dione (101 MHz,  $\text{DMSO-d}_6$ , 298 K).

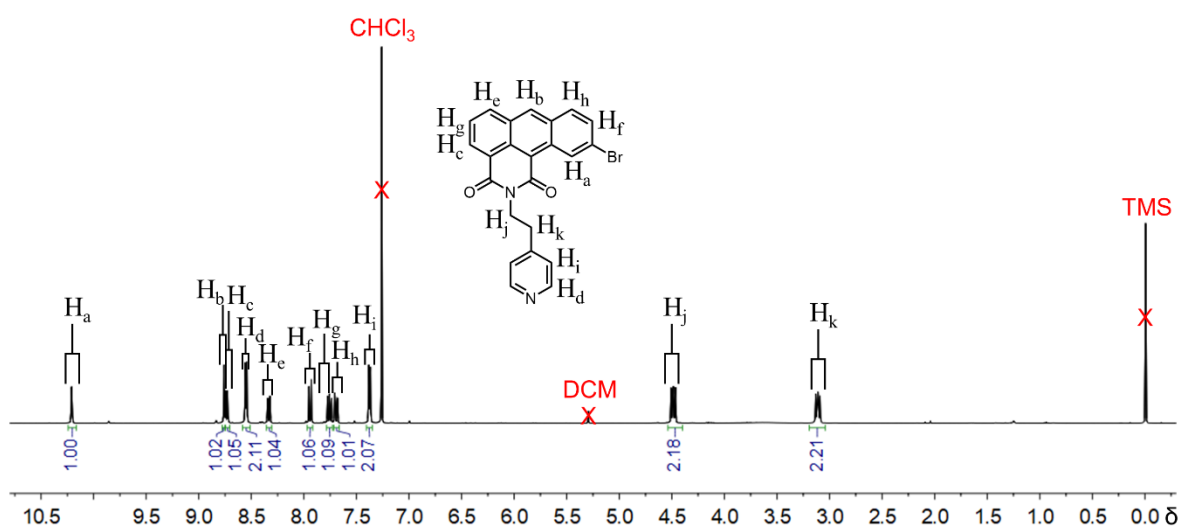


**Figure S23.**  $^1\text{H}$  NMR spectrum of 2AC (400 MHz,  $\text{CDCl}_3$ , 298 K).

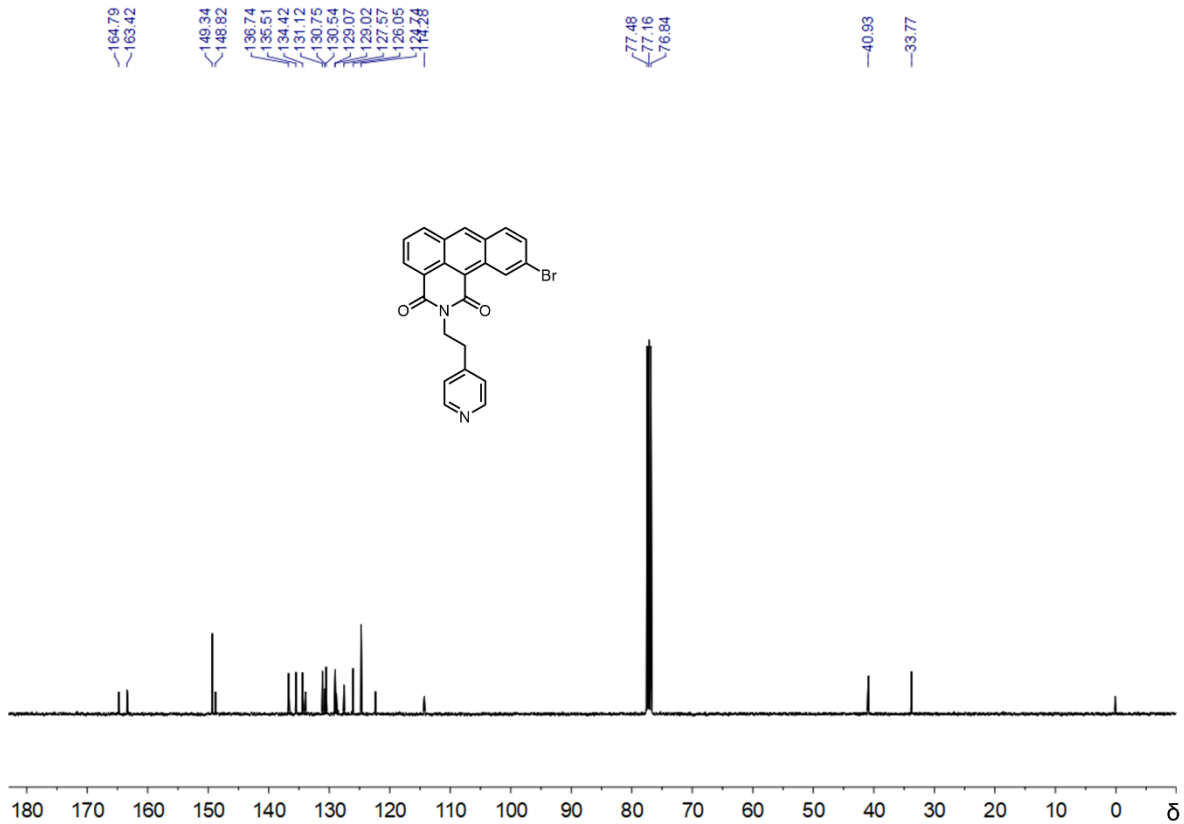


**Figure S24.**  $^{13}\text{C}$  NMR Spectrum of **2AC** (101 MHz,  $\text{CDCl}_3$ , 298 K).

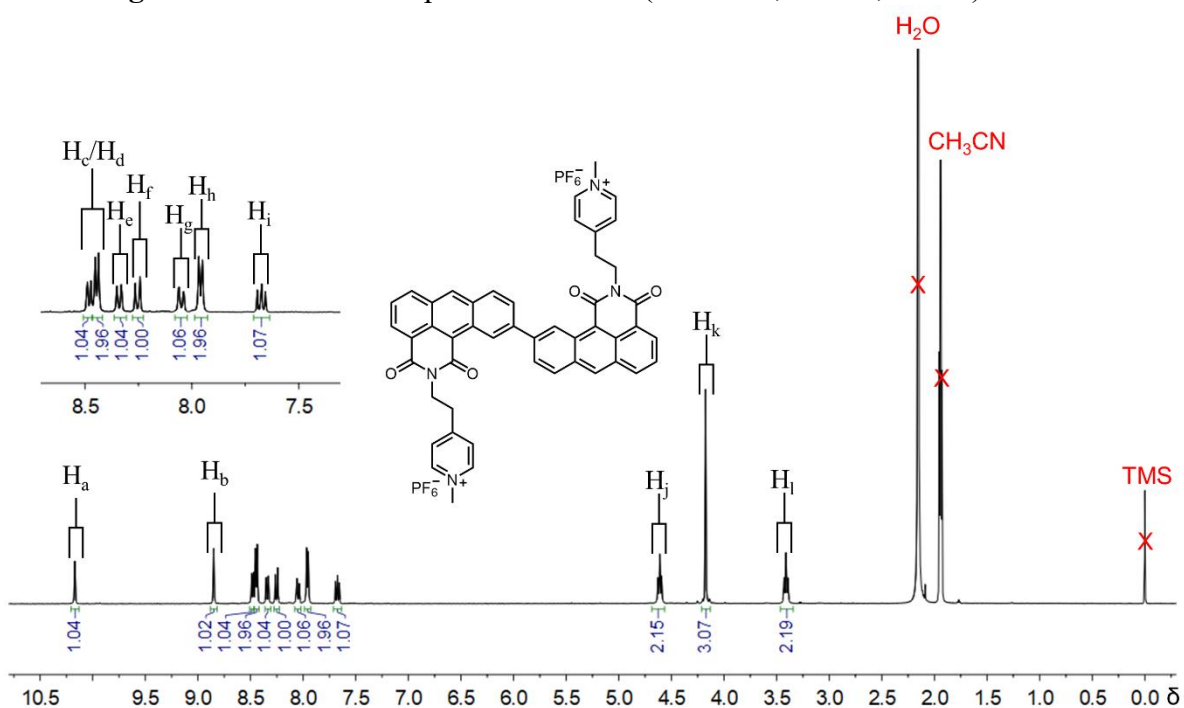


**Figure S25.**  $^1\text{H}$  NMR spectrum of **2DiAC·PF<sub>6</sub>** (400 MHz,  $\text{CD}_3\text{CN}$ , 298 K).

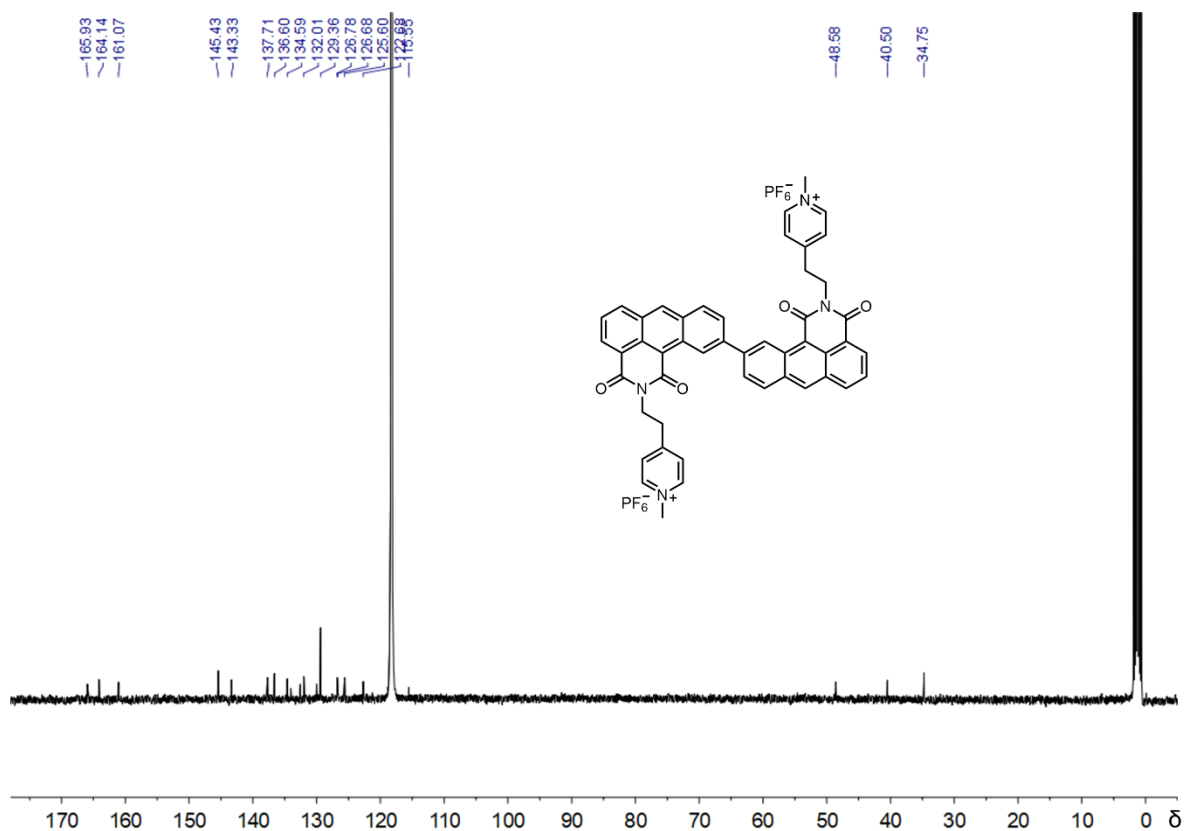


**Figure S26.**  $^{13}\text{C}$  NMR Spectrum of **2DiAC·PF<sub>6</sub>** (101 MHz, CD<sub>3</sub>CN, 298 K).

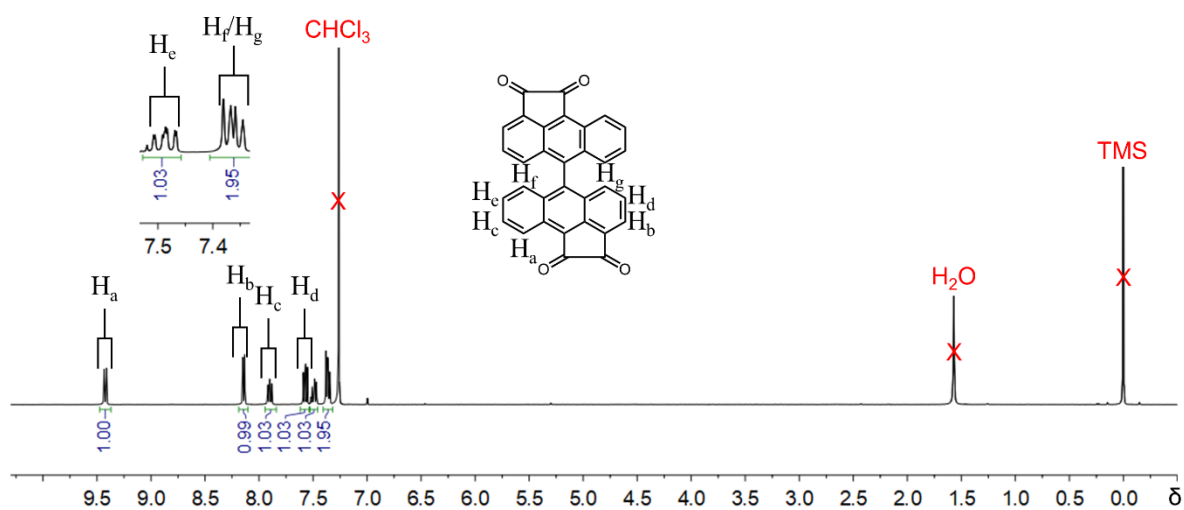


**Figure S27.**  $^1\text{H}$  NMR spectrum of **9DiAn Dione** (400 MHz, CDCl<sub>3</sub>, 298 K).

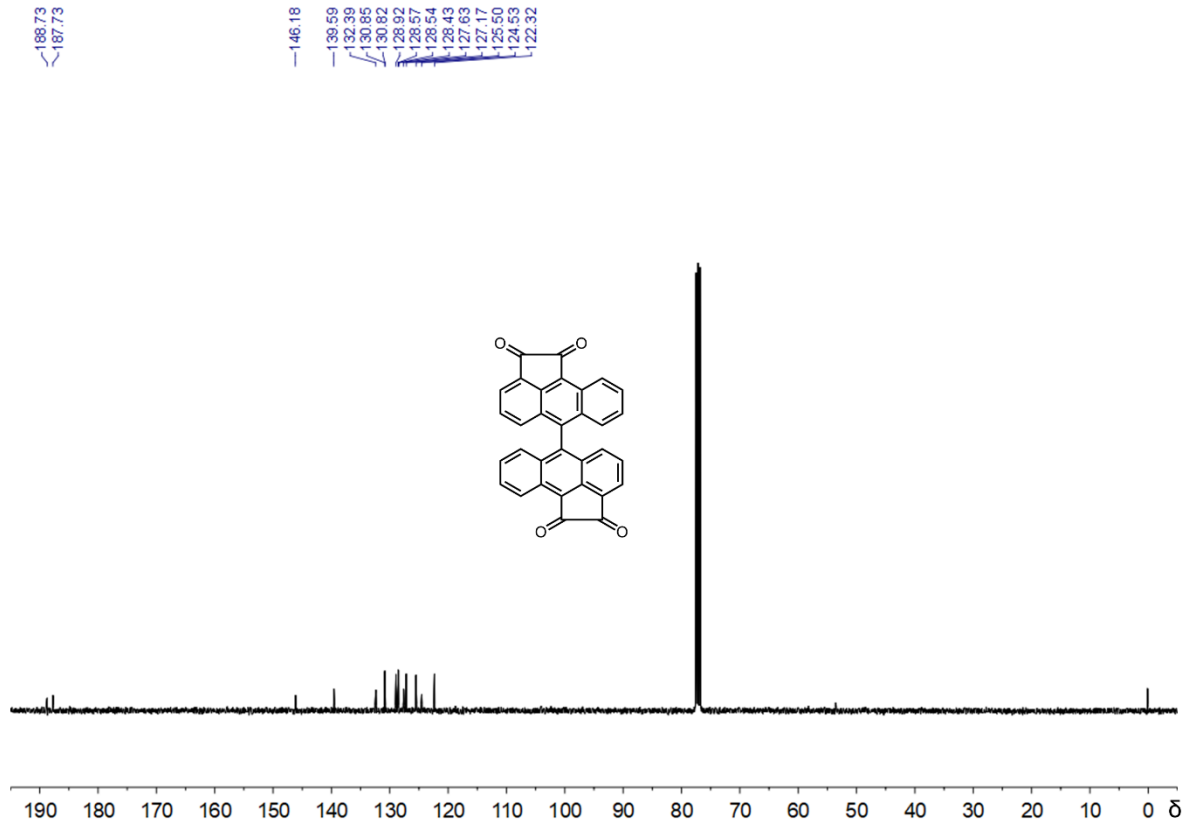


**Figure S28.**  $^{13}\text{C}$  NMR Spectrum of **9DiAn Dione** (101 MHz,  $\text{CDCl}_3$ , 298 K).

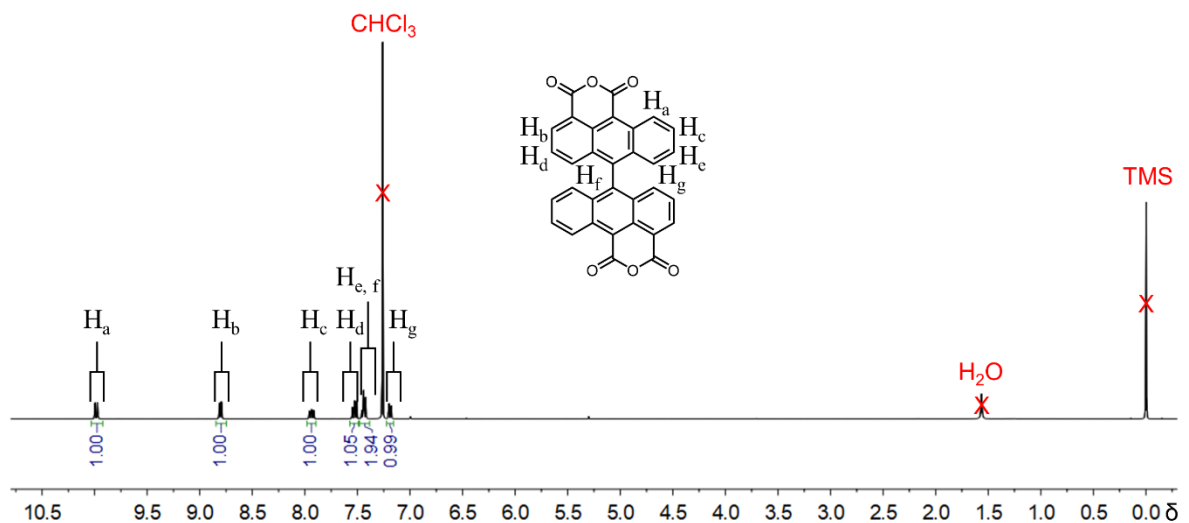


**Figure S29.**  $^1\text{H}$  NMR spectrum of **9DiAn Anhydride** (400 MHz,  $\text{CDCl}_3$ , 298 K).

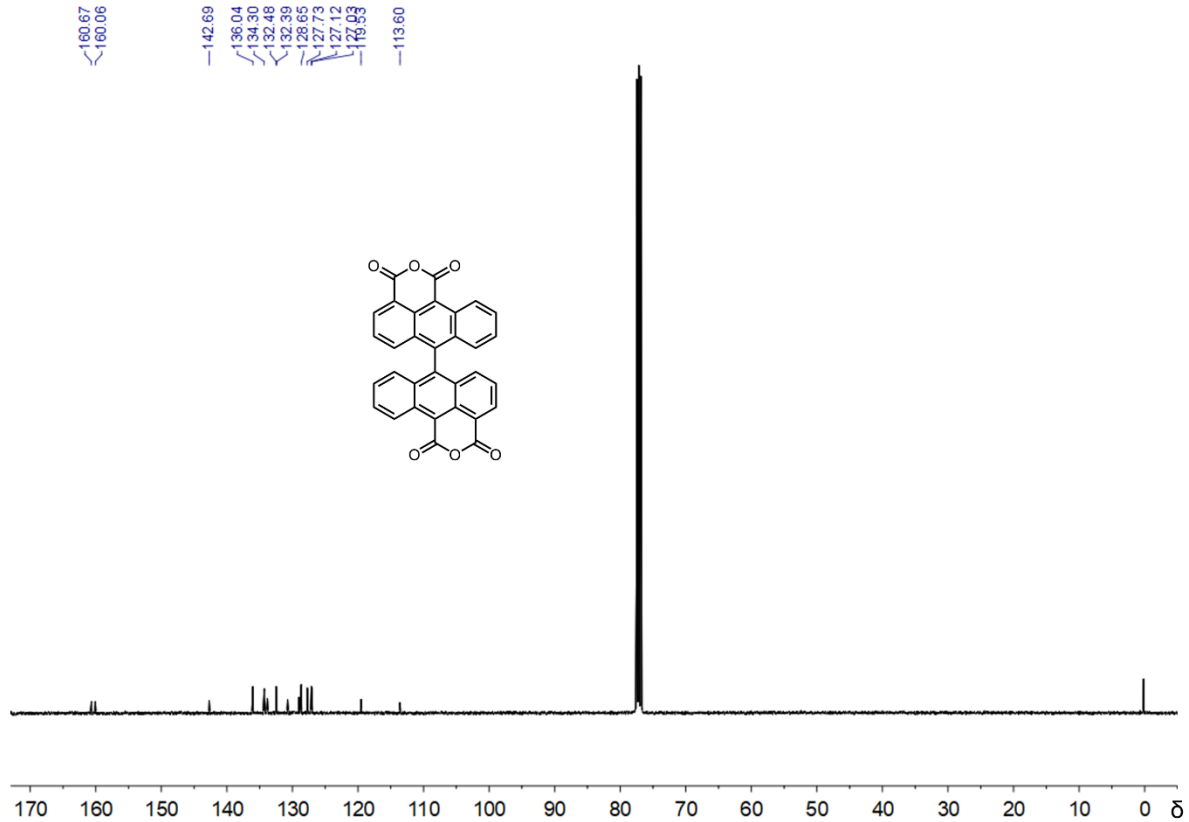


**Figure S30.**  $^{13}\text{C}$  NMR Spectrum of **9DiAn Anhydride** (101 MHz, CDCl<sub>3</sub>, 298 K).

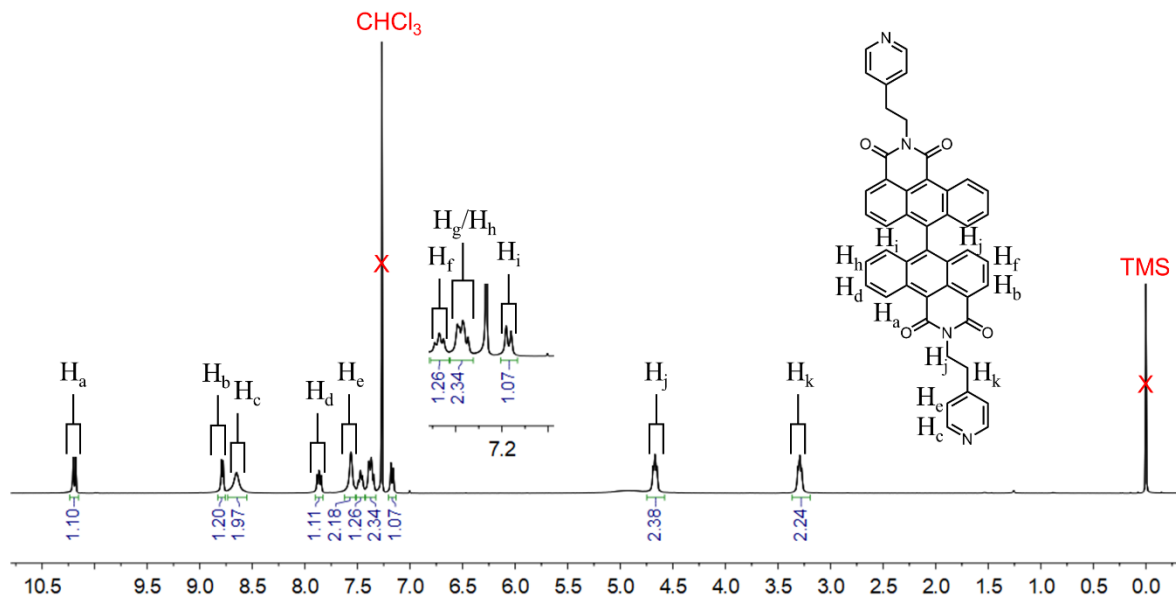


**Figure S31.**  $^1\text{H}$  NMR spectrum of **9DiAC** (400 MHz, CDCl<sub>3</sub>, 298 K).

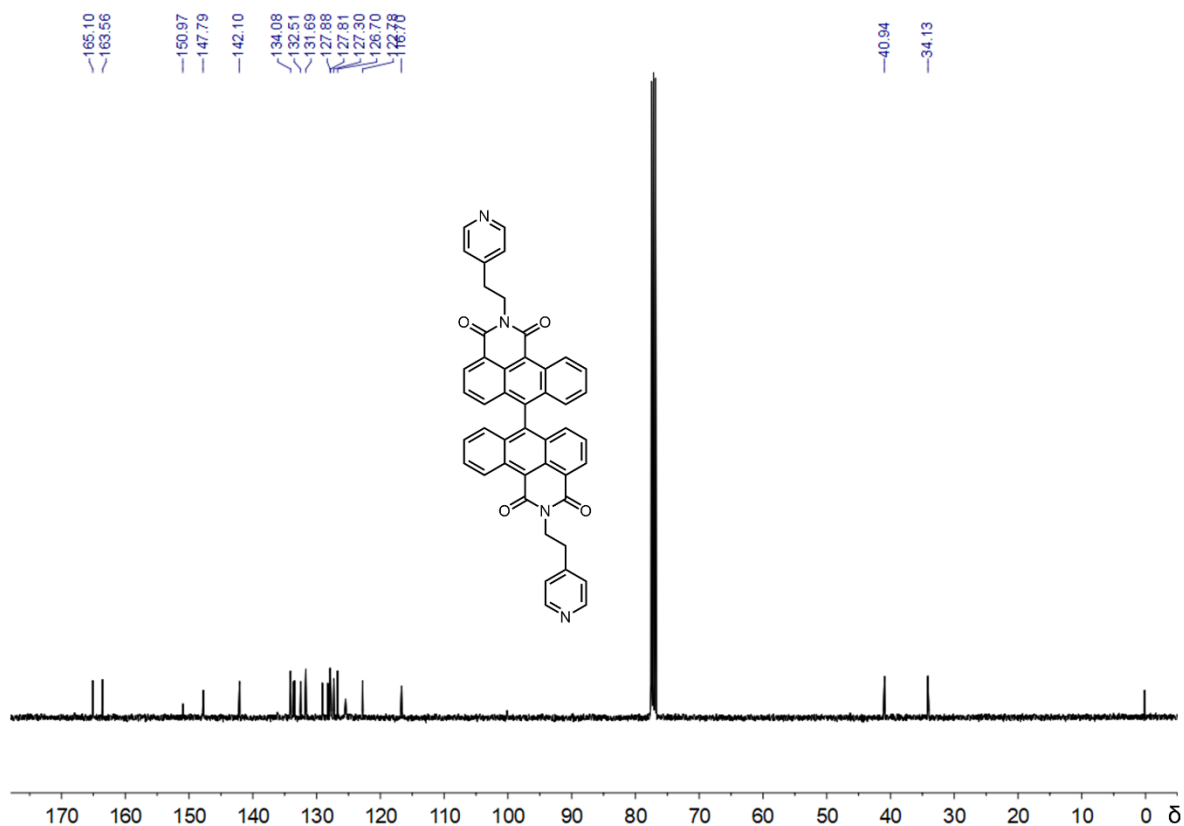


**Figure S32.**  $^{13}\text{C}$  NMR Spectrum of **9DiAC** (101 MHz,  $\text{CDCl}_3$ , 298 K).

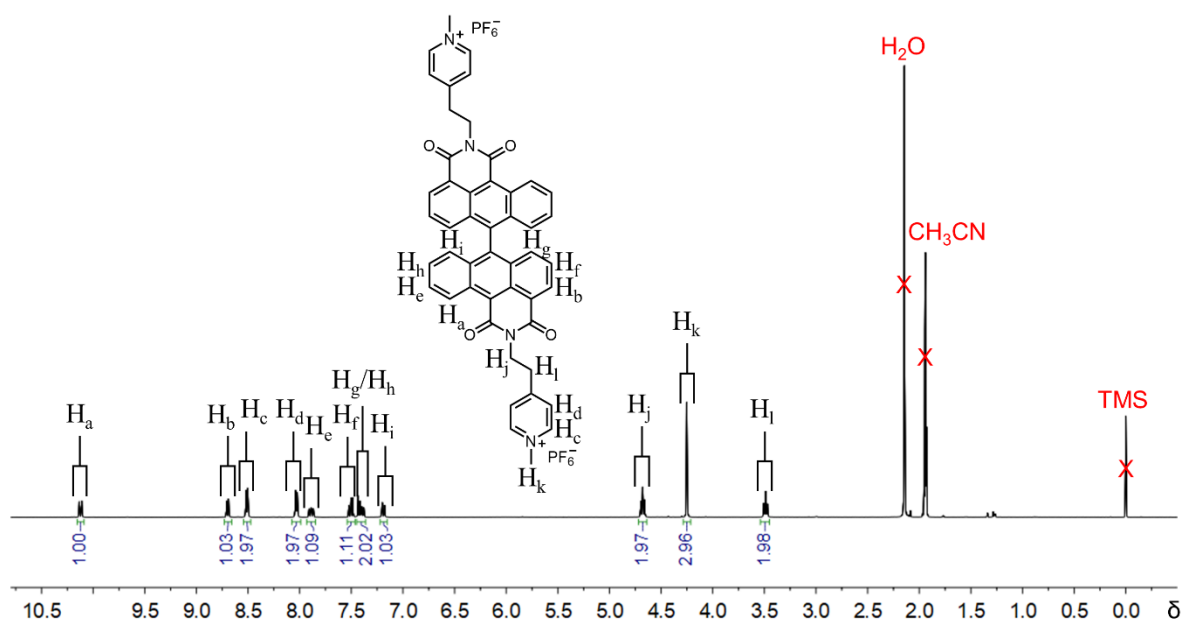


**Figure S33.**  $^1\text{H}$  NMR spectrum of **9DiAC·PF<sub>6</sub>** (400 MHz,  $\text{CD}_3\text{CN}$ , 298 K).

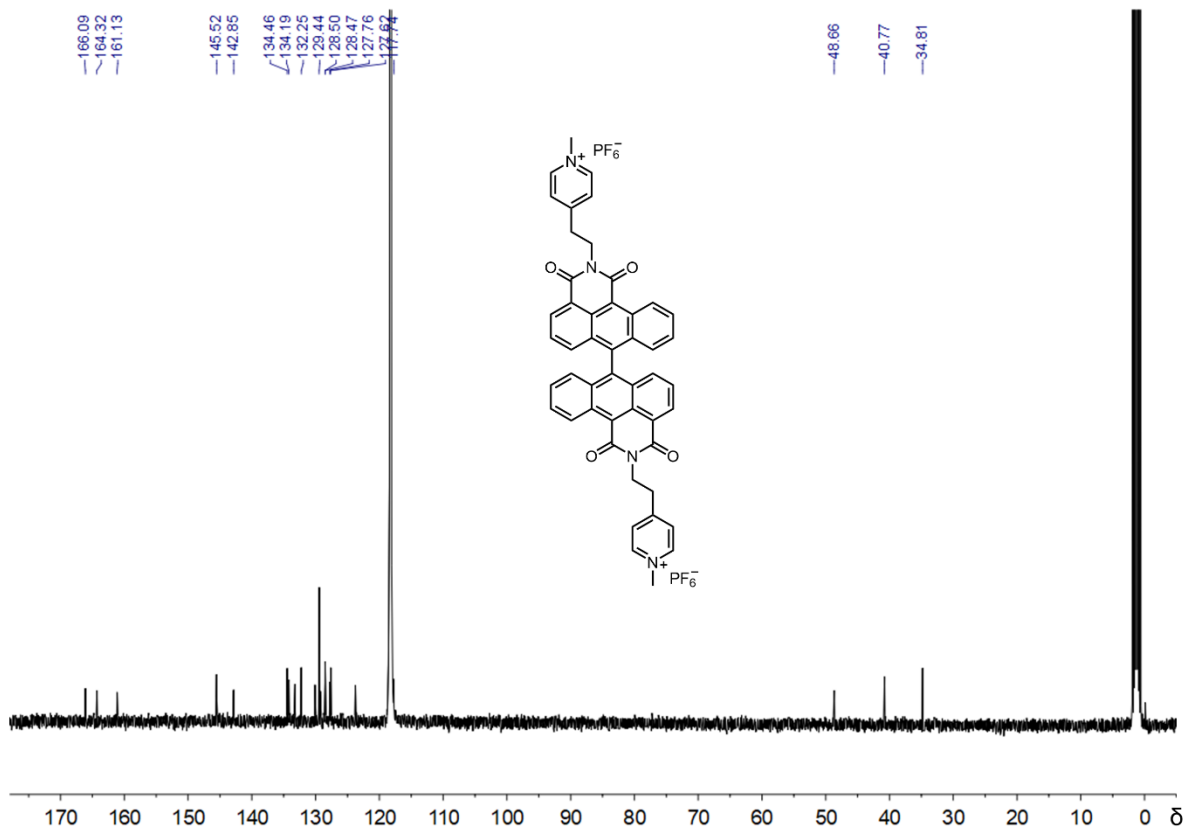


**Figure S34.** <sup>13</sup>C NMR Spectrum of 9DiAC·PF<sub>6</sub> (101 MHz, CD<sub>3</sub>CN, 298 K).

## 8. High Resolution Mass Spectrometry Data

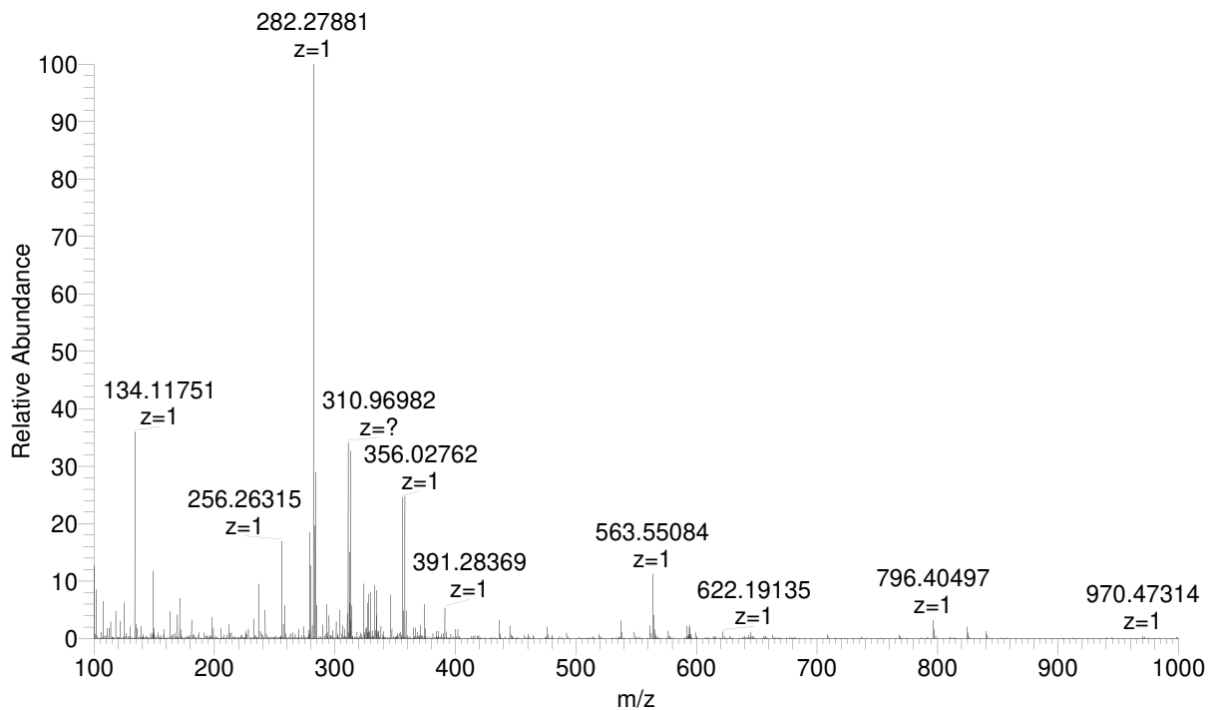


**Figure S35.** High resolution mass spectra of **1An Dione**.

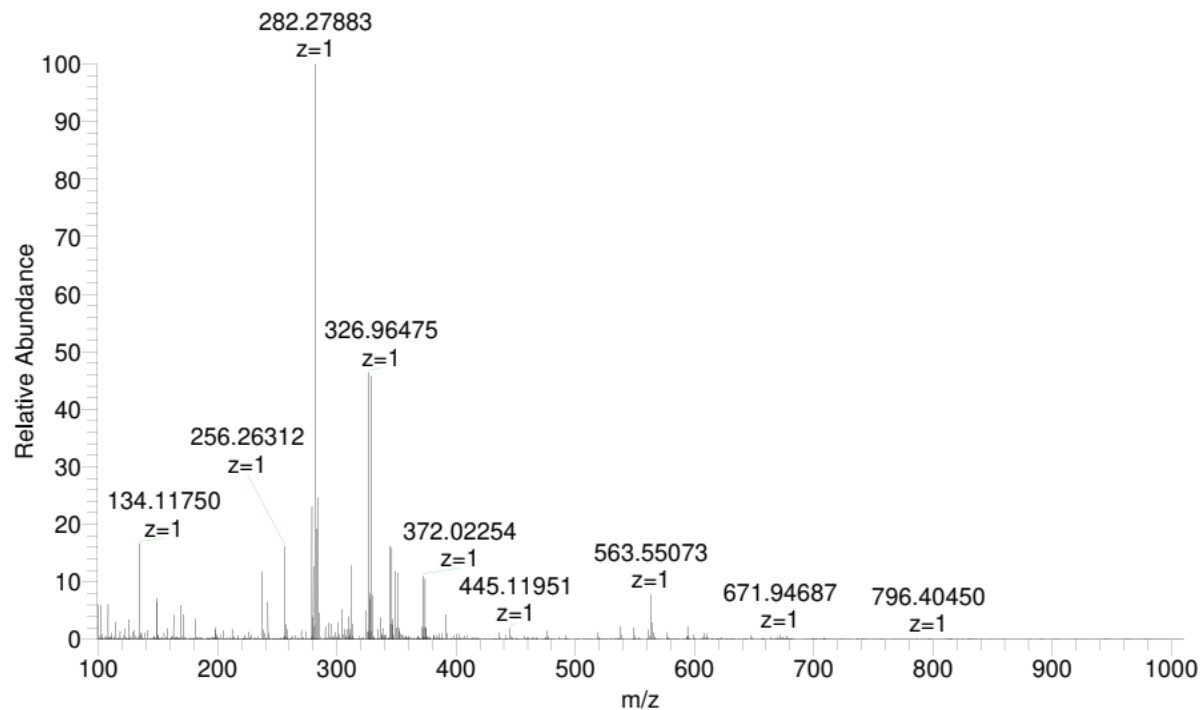


**Figure S36.** High resolution mass spectra of **1An Anhydride**.

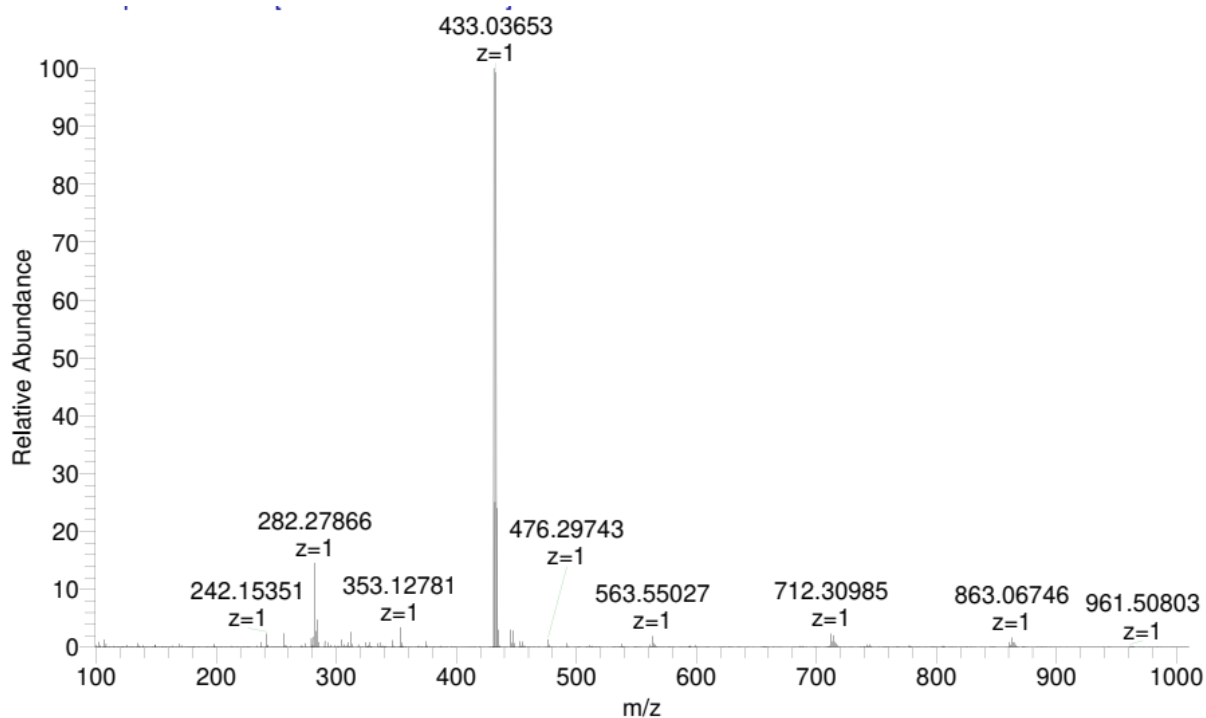


**Figure S37.** High resolution mass spectra of **1AC**.

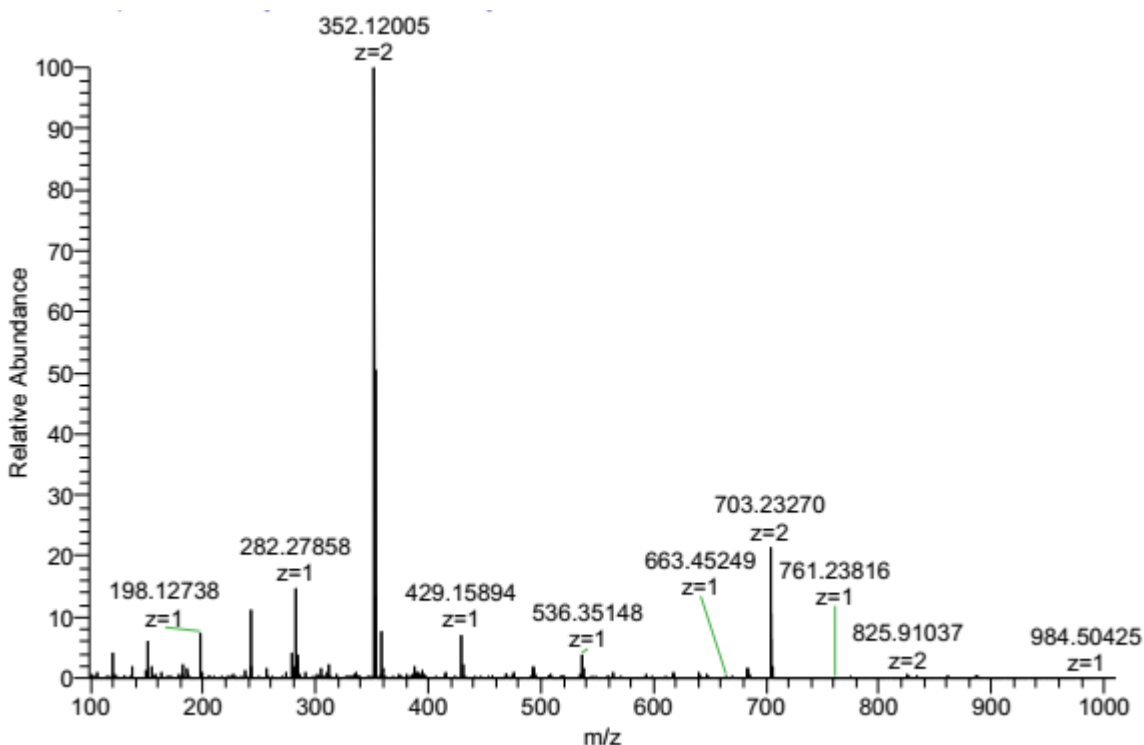


**Figure S38.** High resolution mass spectra of **1DiAC**.

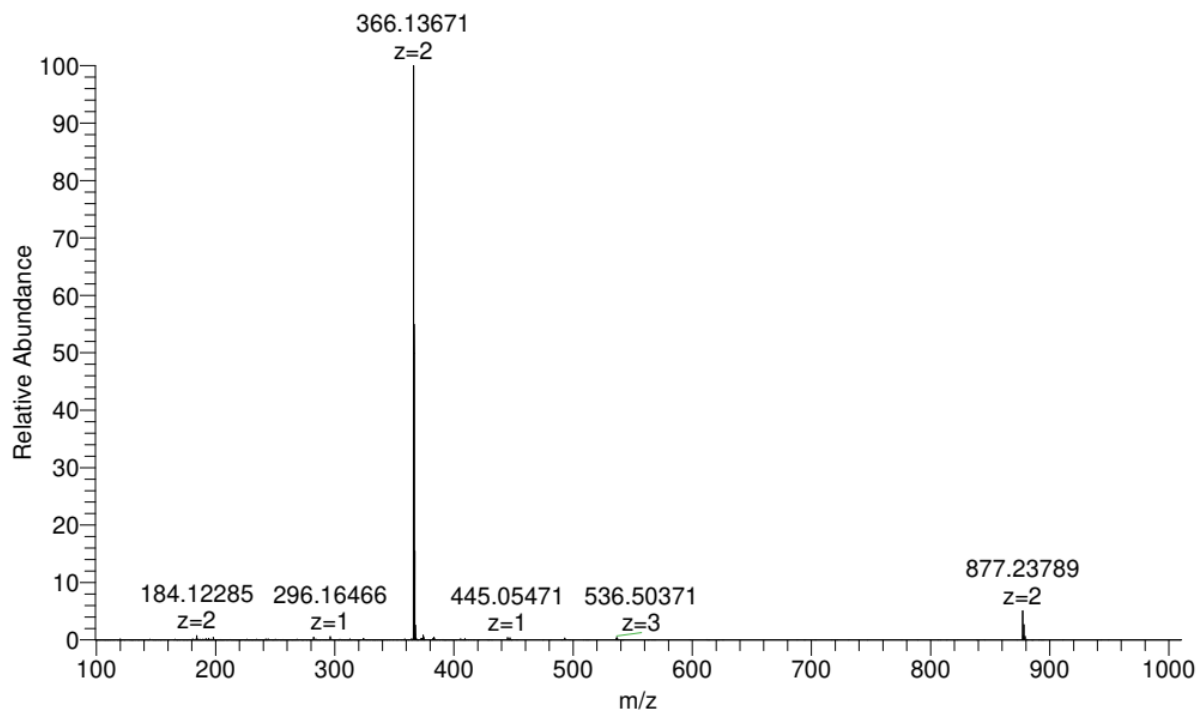


**Figure S39.** High resolution mass spectra of **1DiAC·PF<sub>6</sub>**.

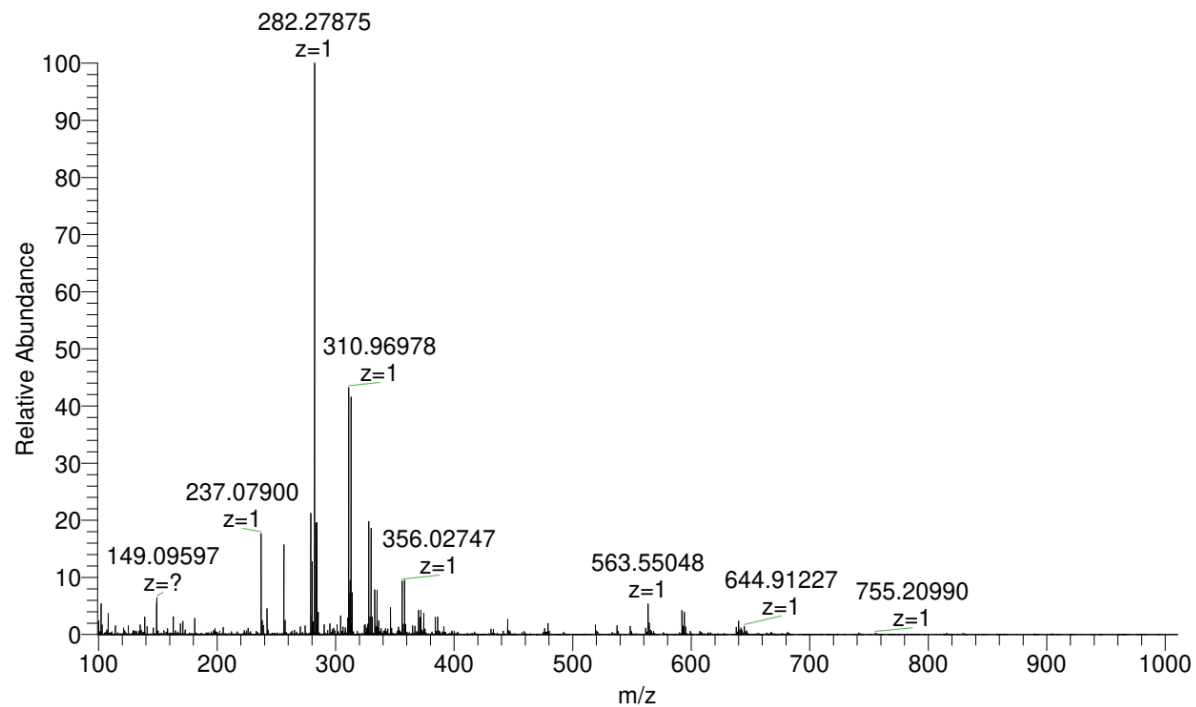


**Figure S40.** High resolution mass spectra of **2An Dione**.

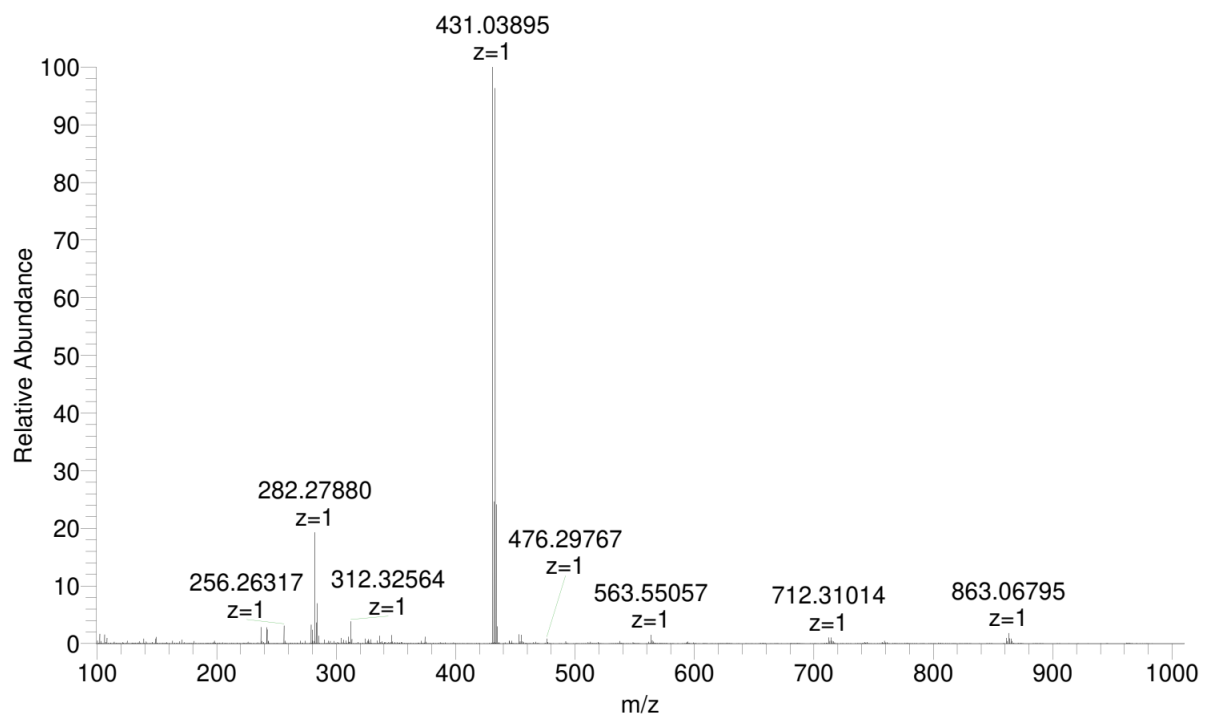


**Figure S41.** High resolution mass spectra of **2AC**.

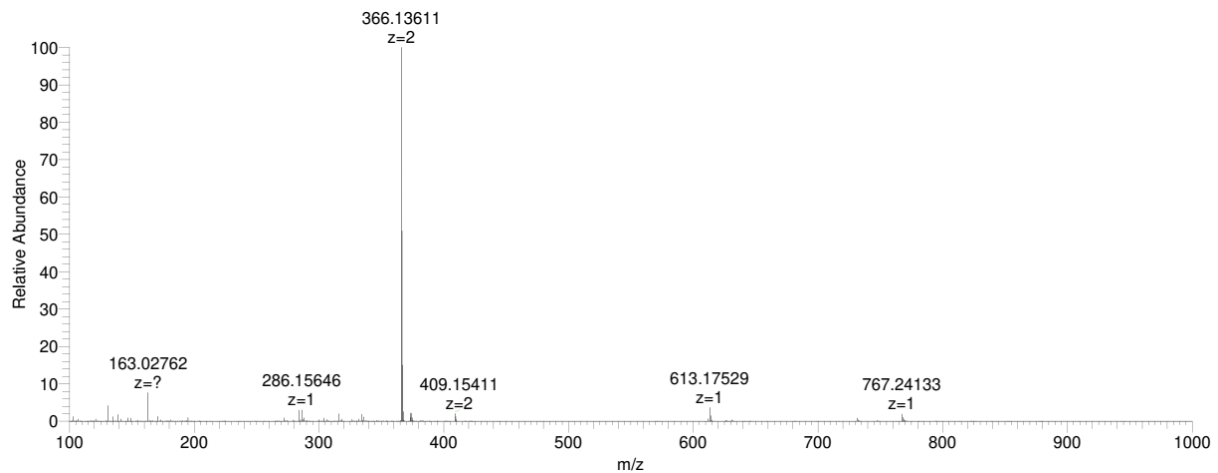


**Figure S42.** High resolution mass spectra of **2DiAC·PF<sub>6</sub>**.

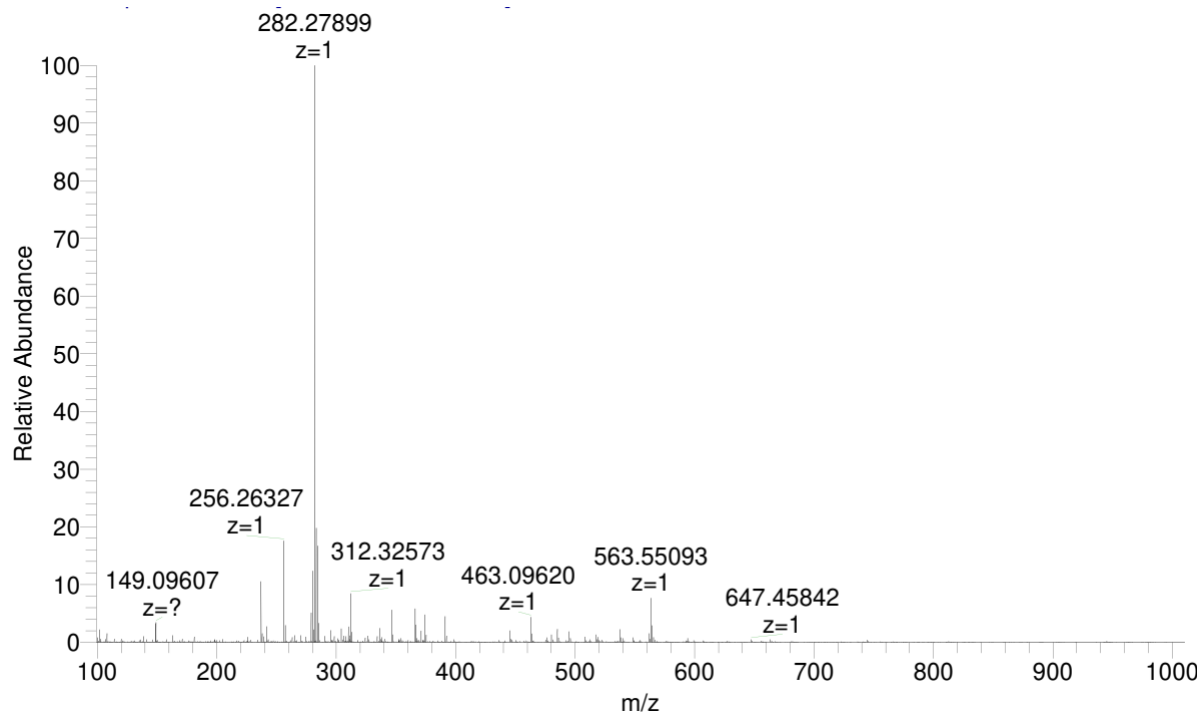


**Figure S43.** High resolution mass spectra of **9DiAn Dione**.

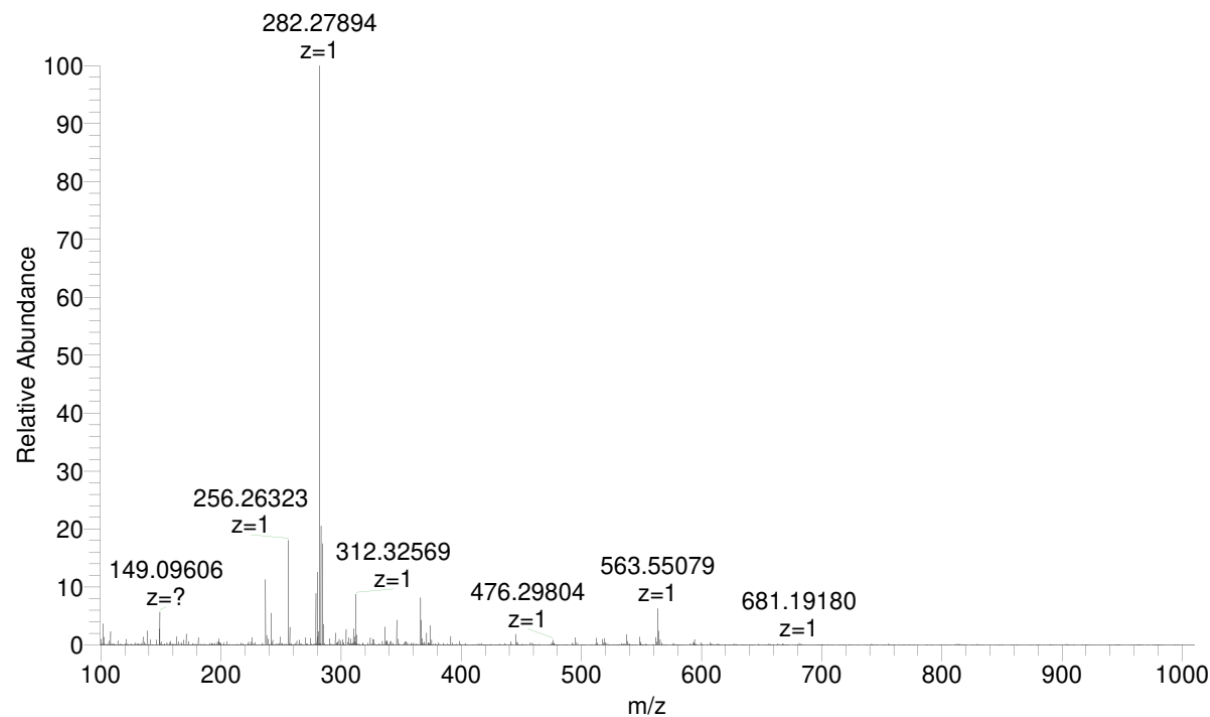


**Figure S44.** High resolution mass spectra of **9DiAn Anhydride**.

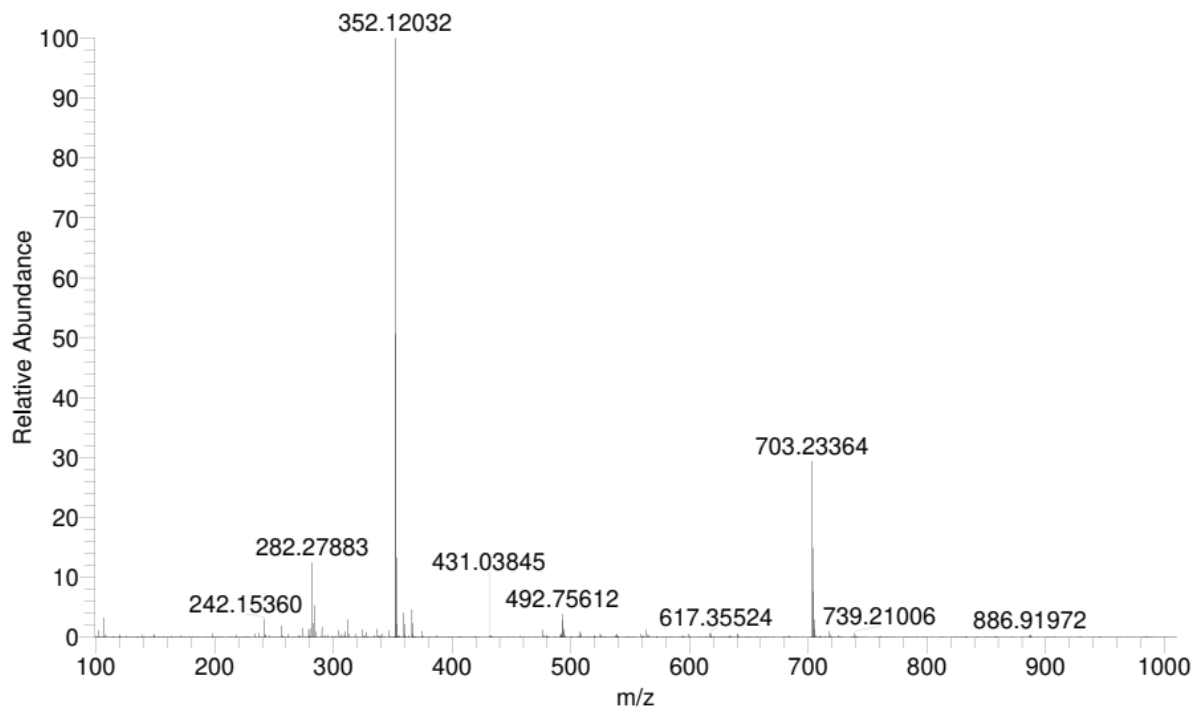


**Figure S45.** High resolution mass spectra of **9DiAC**.

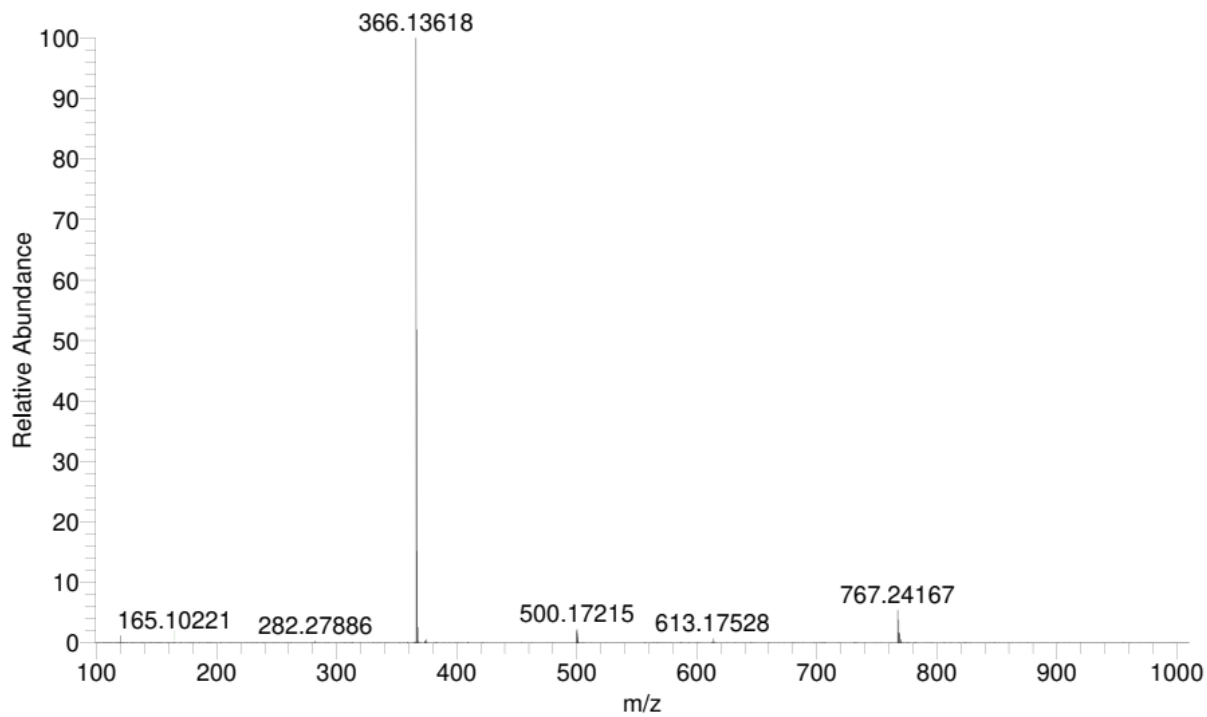


**Figure S46.** High resolution mass spectra of **9DiAC·PF<sub>6</sub>**.

## References

1. Dolomanov, O. V.; Bourhis, L. J.; Gildea, R. J.; Howard, J. A. K.; Puschmann, H. OLEX2: a complete structure solution, refinement and analysis program. *J. Appl. Crystallogr.* **2009**, *42*, 339-341.
2. Sheldrick, G. A short history of SHELX. *Acta Crystallographica Section A* **2008**, *64*, 112-122.
3. GaussView, Version 5, Dennington, R.; Keith, T. A.; Millam, J. M. Semichem Inc., Shawnee Mission, KS, **2016**.
4. T. Lu, F. Chen, Multiwfn: A multifunctional wavefunction analyzer. *J. Comput. Chem.* **2012**, *33*, 580-592.